

Woods Hole Oceanographic Institution

DATA LIBRARY
Woods Hole Oceanographic Institution



A Vector-Averaging Wind Recorder (VAWR) System for Surface Meteorological Measurements in CODE (Coastal Ocean Dynamics Experiment)

by

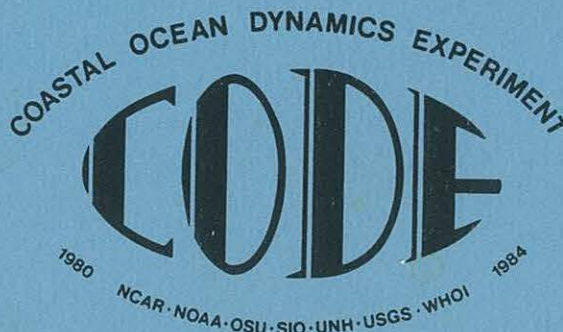
Jerome P. Dean and Robert C. Beardsley

May 1988

Technical Report

Funding was provided by and this report was prepared for the
National Science Foundation under grant
Numbers OCE 80-14941 and OCE 84-17769.

Approved for public release; distribution unlimited.



CODE Technical Report No. 44

WHOI-88-20

**A Vector-Averaging Wind Recorder (VAWR) System
for Surface Meteorological Measurements in CODE
(Coastal Ocean Dynamics Experiment)**

by

Jerome P. Dean and Robert C. Beardsley

Woods Hole Oceanographic Institution
Woods Hole, Massachusetts 02543

May 1988

Technical Report

CODE Technical Report No. 44

Funding was provided by and this report prepared for the
National Science Foundation under grant Numbers
OCE 80-14941 and OCE 84-17769.

Reproduction in whole or in part is permitted for any purpose of the
United States Government. This report should be cited as:
Woods Hole Oceanog. Inst. Tech. Rept., WHOI-88-20.

Approved for publication; distribution unlimited.

Approved for Distribution:

Robert C. Beardsley

Robert C. Beardsley, Chairman
Department of Physical Oceanography



DEVELOPMENT OF A VECTOR-AVERAGING WIND RECORDER (VAWR) SYSTEM
FOR SURFACE METEOROLOGICAL MEASUREMENTS IN CODE
[COASTAL OCEAN DYNAMICS EXPERIMENT]

CONTENTS

	Page
LIST OF FIGURES	ii
LIST OF TABLES	vi
ABSTRACT	vii
1. INTRODUCTION	1
2. THE BASIC VACM OR VAWR DATA RECORDER	9
3. WIND SPEED AND DIRECTION	13
4. AIR AND WATER TEMPERATURE	20
5. INSOLATION	27
6. BAROMETRIC PRESSURE	33
7. RELATIVE HUMIDITY	38
8. INTERCOMPARISONS	41
9. SYSTEM SPECIFICATIONS	67
10. CONCLUSIONS	70
11. ACKNOWLEDGMENTS	72
12. REFERENCES	73

LIST OF FIGURES

Page

4. Figure 1. Locations of WHOI VAWRS deployed in CODE-1 (left) and CODE-2.
5. Figure 2. CODE-1 buoy C-3 meteorological instrumentation. Modified Gill cup and vane sensor set on right, EG&G VMCM modified to function as a Vector Measuring Wind Recorder (WMWR) on the left, with the glass-dome and Thaller-type radiation shields for air temperature on the lower right.
7. Figure 3. CODE-2 buoy C-3 meteorological instrumentation shown during blocked-vane alignment calibration tests on the dock before deployment. The standard wind sensor set is the one on the left and the pyranometer is on the far left. Thaller-type multiplate shields for relative humidity (center, left) and air temperature, and a two-plate port for the barometric pressure sensor are in the center of the photo. An Integral VAWR is on the upper right.
11. Figure 4. Block diagram of the CODE VAWR sensor and data logger system.
12. Figure 5. Tower of the C5 meteorological buoy deployed in CODE-2 with all sensors. These are the pyranometer and barometric pressure port on the left, anemometer and wind-vane in the upper center, and the multiplate radiation shields for temperature (upper right) and relative humidity.
14. Figure 6. Section view of the Standard Gill VAWR cup anemometer and wind-vane assembly.
15. Figure 7. Exploded view of the cup anemometer assembly.
16. Figure 8. Exploded view of the wind-vane assembly.
18. Figure 9. Assembly drawing of the integral cup and vane.
19. Figure 10. Exploded view of the Integral VAWR sensor set.
21. Figure 11. Exploded view of the Thaller-type multiplate radiation shield and air temperature sensor.
22. Figure 12. Section view of the water temperature sensor and its protective housing.
23. Figure 13. Simplified block diagram of the typical temperature channel of the multiplexed VAWR.

25. Figure 14. The dome-shaped radiation shield (right) and the Thaller shield mounted on the C-3 buoy tower for CODE-1.
28. Figure 15. Simplified block diagram of the insolation circuits.
29. Figure 16. View of an Eppley pyranometer mounted on a CODE buoy tower (left.)
31. Figure 17. Assembly drawing of the Hy-Cal pyranometer and mount, with the amplifier housing.
32. Figure 18. Exploded view of the insolation sensor assembly.
34. Figure 19. Section view of the parallel-plate port for barometric pressure measurements from a buoy. After a design by Gerry Gill (Gill, 1976).
35. Figure 20. Exploded view of the parallel-plate port and sensor housing for barometric pressure measurements.
36. Figure 21. Static pressure error of pressure measurements made with the parallel-plate port of Figures 19 and 20. The plot depicts how the error varies with vertical orientation of the port to the direction of the wind. Pressure difference of 0.1 inch of water equals 0.25 mbars; typical buoy inclination is estimated to be less than 10° . This figure is reproduced from Gill, 1976.
37. Figure 22. Simplified block diagram of the barometric pressure circuits in the VAWR.
39. Figure 23. Simplified block diagram of the relative humidity circuits in the VAWR.
40. Figure 24. Exploded view of the Hy-Cal relative humidity sensor, mounting brackets and radiation shield.
44. Figure 25. Histogram and scatter plots of the wind speed measurements made with the VAWR and VMWR in CODE-1.
45. Figure 26. Histogram and scatter plots of the VAWR and VMWR speed difference versus wind speed in CODE-1.
46. Figure 27. Histogram and scatter plots of the direction differences versus wind speed for the VAWR and VMWR in CODE-1.
47. Figure 28. Time series of speed and direction (rotated as defined in the text) for the VAWR with Gill wind sensor set, the modified VMWR, and the differences in the signals as measured by the two systems in CODE-1

49. Figure 29. Variation of the scale factor with blade thickness for the VMCM or VMWR propeller.
51. Figure 30. Time series of speed and direction (rotated as defined in the text) for the VAWR with Gill wind sensor set, the VAWR with the integral sensor set and the differences in the signals as measured by the two systems in CODE-2.
52. Figure 31. Histogram and scatter plots of the wind speed measurements made with the standard VAWR and Integral VAWR in CODE-2.
53. Figure 32. Histogram and scatter plots of the VAWR and Integral VAWR speed difference versus wind speed in CODE-2.
54. Figure 33. Histogram and scatter plots of the direction differences versus wind speed for the standard VAWR and Integral VAWR in CODE-2.
55. Figure 34. Frequency spectrum of a portion of the C3 Standard VAWR and Integral VAWR wind records from CODE-2.
56. Figure 35. Plots of rotor speed difference ($R_2 - R_1$) and the vector-average speed difference ($S_2 - S_1$) versus wind speed (upper panel), and plots of the differences between vector-average speed (S) and rotor speed (R) for each instrument versus wind speed (lower panel). The subscripts 1 and 2 refer to the Standard and Integral VAWRs respectively. The mean and standard deviation statistics have been computed using a wind speed bin width of 2 m/s and the basic 7 1/2 minute time series for the 10 day period, May 1 through May 10, 1982.
57. Figure 36. Plots of the ratio of vector-average speed to rotor speed for each instrument versus wind speed (upper panel) and the standard deviation of the instantaneous direction fluctuations versus wind speed (lower panel). As in Figure 35, subscripts 1 and 2 refer to the Standard and Integral VAWRs and the statistics have been computed for the time period May 1 - 10, 1982.
60. Figure 37. A naturally ventilated wind-steered radiation shield designed to provide a standard for comparisons of various radiation shields.
61. Figure 38. An eight-day test of radiation shields for air temperature sensors. Shown from bottom to top are time series of (A) air temperature as measured in the R. M. Young aspirated shield, AT, (B) difference between AT and temperature sensed in the shield described in the text as the steered shield, (C) wind speed and (D) insolation.

63. Figure 39. Difference plot of the temperatures measured in the standard shield and aluminum multiplate Thaller shield used in CODE. Wind speed, insolation and temperature difference are shown for a cloudy and a sunny day.
64. Figure 40. Theoretical and measured atmospheric transmittance based on the the CODE-1 insolation data.
66. Figure 41. Theoretical and measured atmospheric transmittance based on the CODE-2 insolation data.

LIST OF TABLES

Page

- 3. Table I. Meteorological instruments in CODE-1 and CODE-2.
- 42. Table II. Wind sensor intercomparison statistics.
- 67. Table III. Sensor and system accuracy specifications for the CODE VAWRs.

ABSTRACT

As part of the Coastal Ocean Dynamics Experiment (CODE) field program, moored buoys were instrumented to measure and record wind speed and direction, air and water temperature, insolation, barometric pressure and relative humidity. Appropriate sensors were selected, necessary modifications to the sensors and existing current meters were made, and Vector Averaging Wind Recorders (VAWRs) were assembled. R. M. Young utility rotor and vane wind sets designed by G. Gill, Paroscientific Digiquartz pressure sensors, Eppley pyranometers and Hy-Cal relative humidity and solar sensors were used in two field experiments. Standard VACM direction and temperature sensors were maintained in the wind recorders. Devices were constructed as needed to protect against measurement errors due to wind, sun and ocean spray. Four W.H.O.I. VAWRs with Gill wind sensor sets were deployed CODE-1 in 1981. Seven VAWRs were deployed in CODE-2 in 1982. A modified VMCM (Vector Measuring Current Meter) was used for comparison in CODE-1, and the seventh VAWR deployed in CODE-2 carried an integral sensor set for comparison. Although several VAWRs had minor problems, all but one VAWR in the two experiments returned useful scientific data.

1. INTRODUCTION

To better understand the interaction and energy exchange between the atmosphere and the ocean and to study the atmospheric mechanisms that drive the upper ocean, one must measure the wind at sea near the ocean surface. A reliable platform and a wind sensor which can survive for time periods of the order of months and remotely record or telemeter continuous data to a shore station are required.

In the early 1970's, engineers at the Woods Hole Oceanographic Institution (WHOI) designed the Vector-Averaging Current Meter (VACM) which has become the standard long-term reliable instrument to provide a continuous measure of ocean current velocity and serve as a data recording instrument for temperature and other variables. This data logging capability and the feature allowing simple modification to change the data format made this current meter an ideal choice for use as a wind recorder. Payne (1974) and Halpern (1974) were the first investigators who converted the VACM into a vector-averaging wind recorder in field experiments conducted in 1972 and 1973, successfully.

Beginning in 1980, the Coastal Ocean Dynamics Experiment (CODE) was undertaken to identify and study the important dynamic processes which govern the wind-driven water motion over the continental shelf and slope off northern California. Two small scale, densely-instrumented field experiments of approximately four-months duration (called CODE-1 and CODE-2) were conducted to obtain high quality data sets of the relevant physical variables needed to construct accurate kinematic and dynamic descriptions of the response of shelf water to strong wind forcing. (See Allen et al. (1982) and the CODE Group (1983) for additional descriptions of the CODE-1 and CODE-2 experiments.) As part of the WHOI component in this field program, it was proposed to deploy moored buoys with meteorological instrumentation to measure and record wind speed and direction, air and water temperature and other variables.

To achieve this objective, appropriate meteorological sensors were selected, necessary modifications were made to sensors and existing VACMs, and wind recorders were assembled. The R. M. Young Company utility wind sensor set consisted of a three-cup anemometer and wind vane which seemed to best meet the criteria

of sensitive yet rugged sensors proven in the field and accepted by the meteorological community. The rotor and vane set had the added advantage of basic compatibility with the VACM which uses a polar system of rotor and vane sensors. Based on the Gill three-cup anemometer design, except constructed of slightly thicker aluminum, the unit was easily mounted on a buoy. The Gill microvane fin was made of aluminum rather than rigid foam, a small sacrifice in sensitivity to provide added durability. The WHOI modification consisted of replacing the anemometer DC generator with a magnetic sensor to drive the VAWR vector computer circuits. The factory supplied potentiometer coupled to the vane shaft was replaced with a digital encoder to supply seven-bit binary vane position information. Neither of these changes was detrimental to performance and, in fact, decreased the mechanical friction component normally present in the sensors.

Four WHOI VAWRs with Gill utility wind sensor sets were deployed in the first small-scale experiment (CODE-1) conducted in 1981. Figure 1 is a location map showing the four sites. These VAWRs were instrumented to measure and record east and north wind velocity components, air and seawater temperature and insolation (incident solar radiation) (see Table I). Air and water temperature were sensed with thermistors and insolation was measured with hot-and-cold-junction thermopile pyranometers. In CODE-1, two types of air temperature radiation shields were used to protect the air temperature sensors from unwanted radiation heating. One was an off-the-shelf glass dome shield modified to help protect against reflected radiation, and the second was an aluminum Thaller-type multiplate shield. Both air temperature radiation shields and the wind sensor sets mounted on the C3 toroid are shown in Figure 2.

Comparison was also made between the VAWR with the Gill wind sensors and a version of the then new EG&G Vector Measuring Current Meter (VMCM) mounted as a wind recorder on the C3 buoy. The standard current meter sensors of this dual propeller instrument were replaced with lighter propeller sensors made of acetal plastic (Delrin). The sensor bearings failed after about one month but a useful intercomparison was achieved. An early version of the Vector Measuring Wind Recorder (VMWR) made from an Scripps Institution of Oceanography (SIO) VMCM was used in the Joint Air-Sea Interaction (JASIN) experiment in 1978, when similar problems were encountered (Weller et al., 1983).

Table I

Meteorological Instrumentation deployed in Code-1 and Code-2

CODE-1 (April - August, 1981)

CODE (Sta.) Location	VAWR #	Wind Sensor	Sea Temp.	Air	Ref	Insol.	RH	BP
C3B (709)	V121W	Gill	X	X	X	X		
C1B (708)	V139W	Gill	X	X	X	X		
R3B (711)	V141W	Gill	X	X	X	X		
C5B (710)	V182W	Gill	X	X	X			
C3B (709)	VM301	VMCM						

CODE-2 (April - August, 1982)

R3B (751)	V121W	Gill	X	X		X		
N3B (756)	V139W	Gill	X	X		X		
C2B (752)	V141W	Gill	X	X				
C5B (758)	V161W	Gill	X	X		X	X	X
C3B (753)	V177W	Gill	X	X		X	X	
C4B (760)	V182W	Gill	X	X		X		
C3B (753)	V381W	Integral						X

Ref: Reference channel for circuit stability

RH: Relative Humidity

BP: Barometric pressure

Sta.: WHOI Moored station number

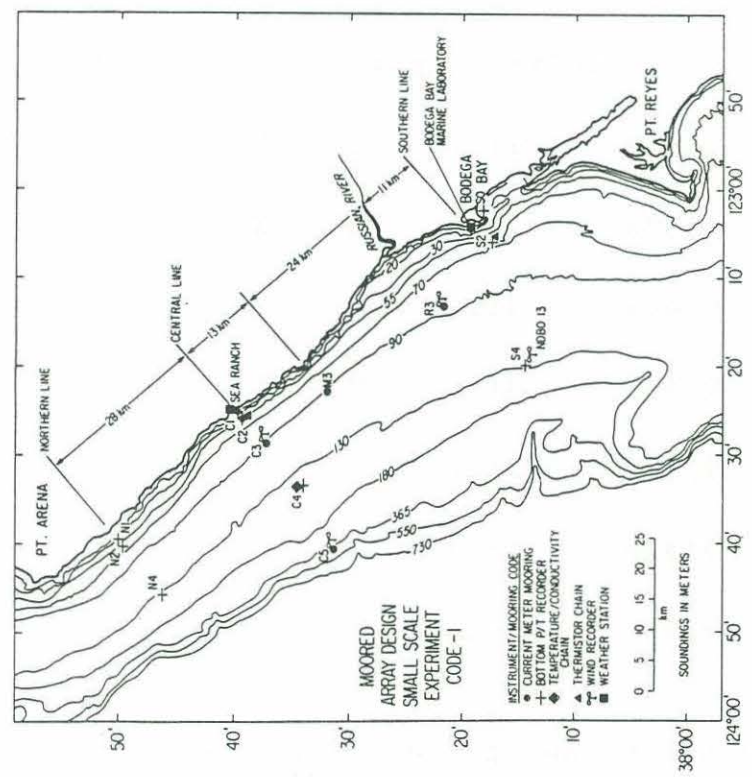
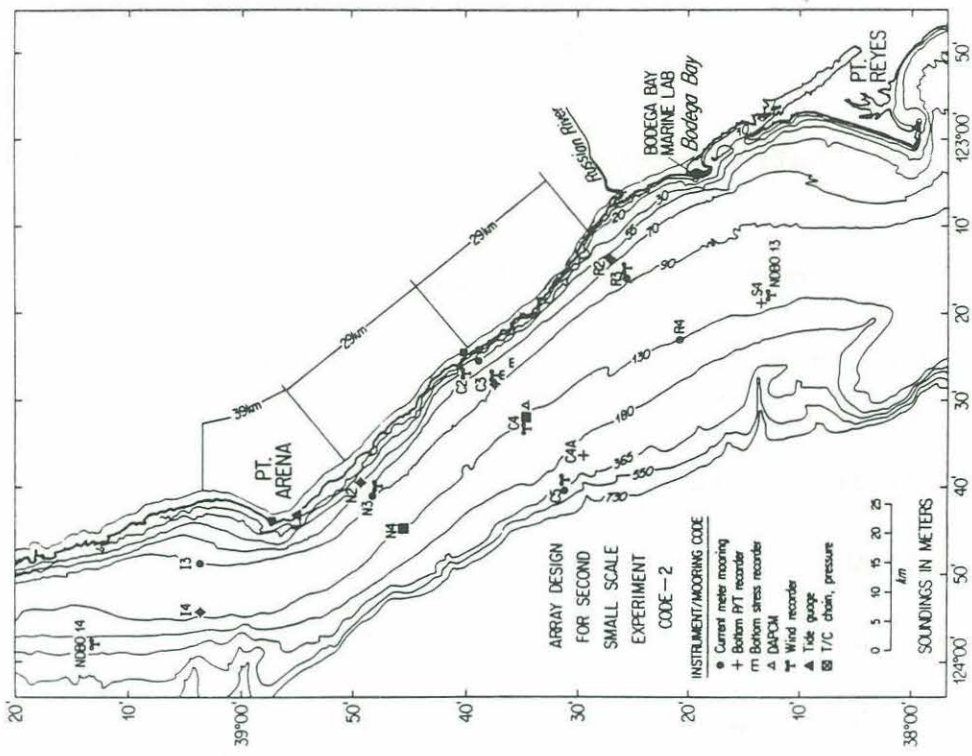


Figure 1. Locations of WHOI VAWRS deployed in CODE-1 (left) and CODE-2.

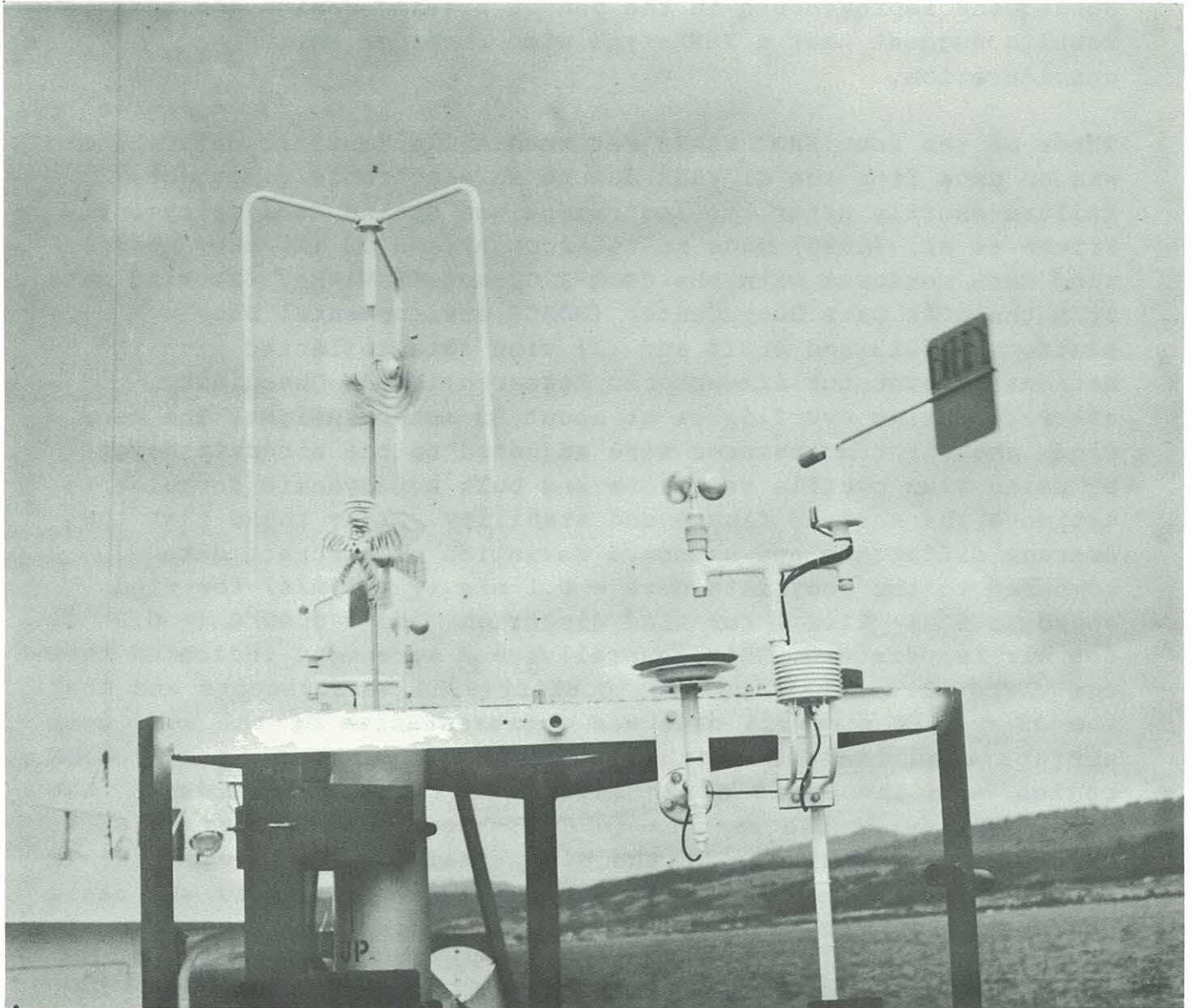


Figure 2. CODE-1 buoy C-3 meteorological instrumentation. Modified Gill cup and vane sensor set on right, EG&G VMCM modified to function as a Vector Measuring Wind Recorder (WMWR) on the left, with the glass-dome and Thaller-type radiation shields for air temperature on the lower right.

Subsequent improvements in the sensor bearing design and test results suggest that a VMWR-type wind recorder merits consideration.

Three of the four WHOI VAWRs returned all scientific data. There was no data from the C1 VAWR due to an electronic component failure shortly after the instrument was sealed for deployment. Friehe et al. (1984) made an intercomparison of (1) buoy vector wind data measured with the CODE-1 C3 and C5 VAWRs, (2) wind data from the NOAA Data Buoy Center (NDBC) environmental buoy platforms 46013 and 46014 and (3) wind data collected with the National Center for Atmospheric Research (NCAR) Queen Air aircraft during overflights at about 33 meters height. The buoy winds and air temperatures were adjusted to the aircraft height by using flux profile relations and bulk aerodynamic formulae to estimate the surface fluxes and stability. They found that the average difference and standard deviation of aircraft data compared to the buoy data were + 0.1 m/s (± 1.8 m/s) for wind speed, 3.3° ($\pm 11.2^\circ$) for wind direction, and + 0.02°C ($\pm 0.2^\circ$ C) for air temperature. This generally good agreement indicated that the VAWRs were obtaining high quality wind measurements and that the 33 m NCAR aircraft data was representative of the very near surface wind field beneath the marine inversion in the CODE region. On the basis of this favorable intercomparison, the survivability of the sensors in CODE-1 and other tests at WHOI, the overall performance of the Gill utility cup and vane set in the field was deemed satisfactory and the same sensors and basic configuration with some additions were used the next year in CODE-2.

A total of six WHOI VAWRs with Gill wind sensors were deployed in CODE-2 in 1982. (See Figure 1 for the VAWR deployment positions in CODE 2). All VAWR systems measured air and sea temperature; some instruments measured insolation, relative humidity and barometric pressure (see Table 1). In addition, a seventh VAWR with an integral vane-follower was deployed for redundancy and for comparison with the standard Gill wind sensor set. The integral VAWR used the Gill-type cup set mounted atop a three-legged protective support or cage. The wind vane was mounted directly below the cups inside the cage as shown on the right in Figure 3. The vane was magnetically coupled to a VACM vane follower, a seven-bit digital encoder located inside the cylindrical electronics housing. This design provided an integral assembly requiring no special alignment of vane and

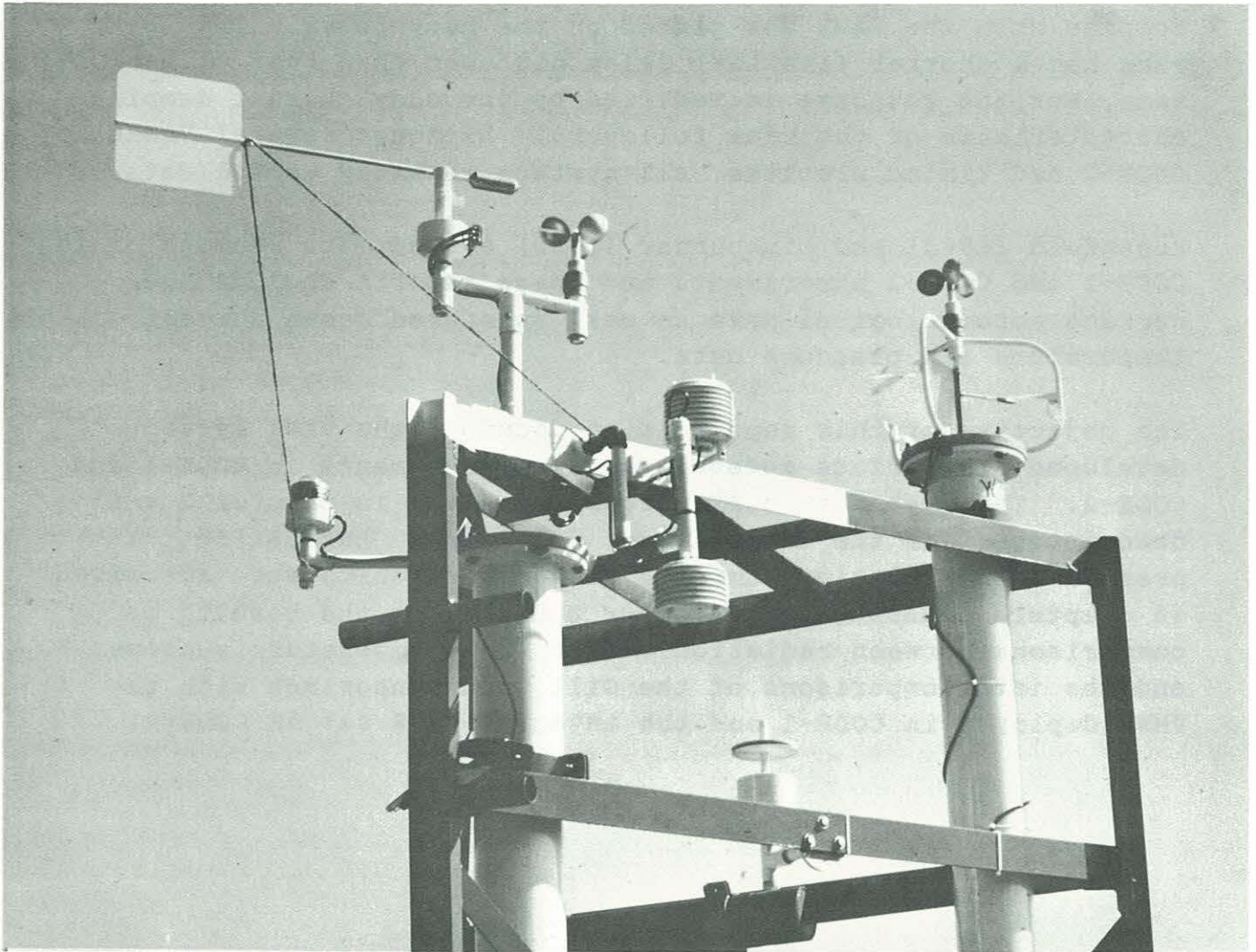


Figure 3. CODE-2 buoy C-3 meteorological instrumentation shown during blocked-vane alignment calibration tests on the dock before deployment. The standard wind sensor set is the one on the left and the pyranometer is on the far left. Thaller-type multiplate shields for relative humidity (center, left) and air temperature, and a two-plate port for the barometric pressure sensor are in the center of the photo. An Integral VAWR is on the upper right.

compass when the VAWR was placed on the buoy tower. (This wind vane has a shorter (smaller) delay distance than that of the Gill vane, but the response is modified by the eddy current damping characteristic of the vane follower.). Although several VAWRs in CODE-2 had timing problems, all systems returned useful data.

Roesnfeld (1983) and Limeburner (1985) edited data reports of the CODE-1 and CODE-2 experiments and these reports include the surface meteorological data as well as moored ocean current, temperature and pressure data.

The objective of this report is to document the VAWR system developed for surface meteorological measurements in CODE-1 and CODE-2. The system specifications are given in Chapter 2 and descriptions of the temperature, insolation, barometric pressure, and relative humidity sensors, circuits etc. are given in Chapters 3 through 7. Chapter 8 describes the results of comparisons between radiation shields for temperature sensors, and the intercomparisons of the Gill wind sensor set with the VMWR deployed in CODE-1 and the integral VAWR set in CODE-2.

2. THE BASIC VACM OR VAWR DATA RECORDER

In the early 1970's, engineers at WHOI developed a vector-averaging current meter now commonly known as the VACM (McCullough, 1974). The VACM sums vector increments of water displacement in geographic co-ordinates as sensed by a Savonius rotor, a magnetic compass and a water directed vane. At regular preset intervals, usually 7 1/2 or 15 minutes, the VACM records the accumulated magnetic North (u) and East (v) vectors, an instantaneous position of the compass and vane, total rotor revolutions, an average temperature for the interval and a record count, commonly known as the clock. The tape recorder developed for the VACM has the capacity for recording additional data when used for less than 500 days recording 15 minute averages. There is room for additional circuitry and reserve battery power available for shorter experiments. By 1980, a modification had been developed which allowed temperature and up to three additional parameters to be recorded in a time-shared or multiplexed mode. Pressure and temperature are commonly recorded in the modified VACMs (known at WHOI as a multiplexed VACM), and four temperatures were recorded in a bottom boundary layer experiment in 1978. The two extra channels are sometimes used to measure the inclination of the meter, thus the mooring, at that depth.

Modification of a multiplexed VACM into a VAWR was relatively straightforward. Wind sensors were modified to provide appropriate signals to the vector computer circuits, and shields were bought or made to protect the temperature sensing thermistors from unwanted heating by short and longwave radiation. The multiplexing circuits were used to record the air and sea temperatures and circuits were devised to interface pyranometer (insolation), barometric pressure and relative humidity signals into the data record of some VAWRS. A two-plate port (Gill, 1976) was built to interface the pressure sensor to the atmosphere and reduce the effects of the wind and buoy motion on the measurement. Strain gauge relative humidity transducers, which were compatible with the VACM multiplex circuits, were used with mixed success; these sensors also required radiation shields.

An overall system block diagram is shown in Figure 4. Figure 5 is a photograph of the tower of the toroid buoy moored at C-5 during CODE-2. This was the only instrument modified to include

all parameters and is shown on the dock during preparations for the experiment. The individual sensors and components are described more fully in the following sections.

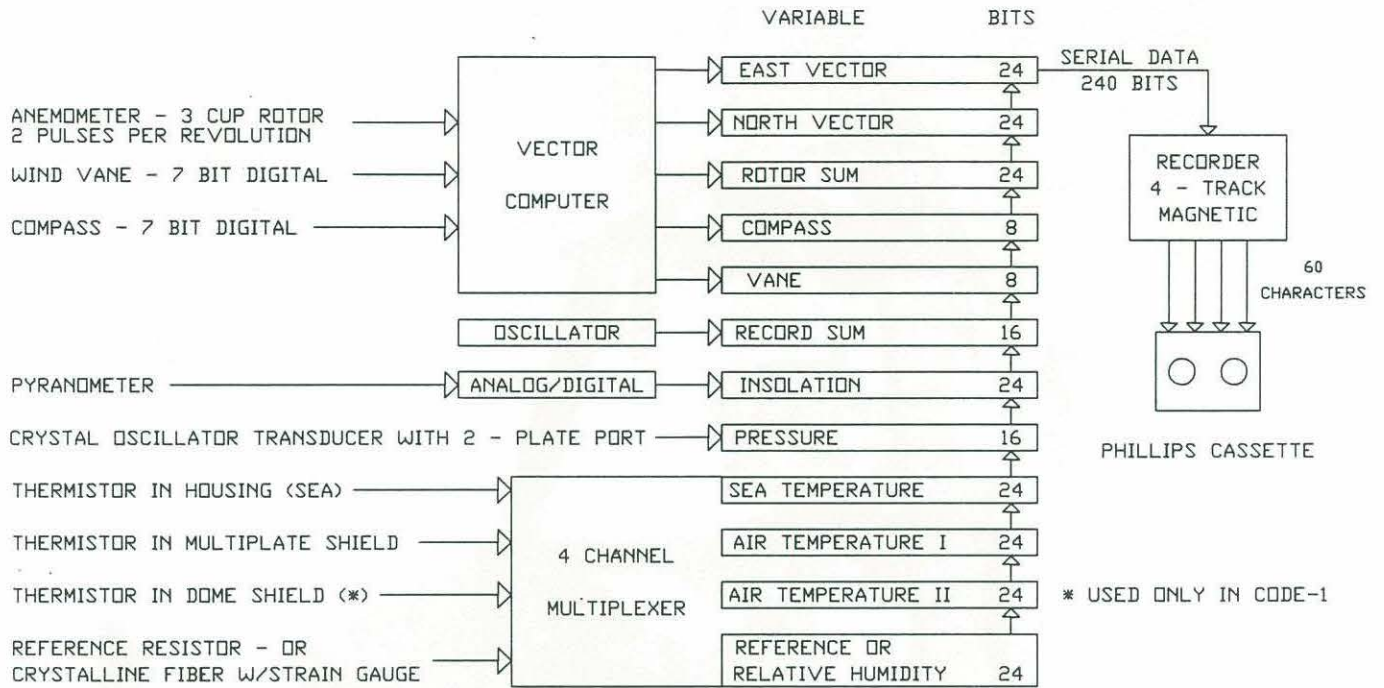


Figure 4. Block diagram of the CODE VAWR sensor and data logger system.



Figure 5. Tower of the C5 meteorological buoy deployed in CODE-2 with all sensors. These are the pyranometer and barometric pressure port on the left, anemometer and wind-vane in the upper center, and the multiplate radiation shields for temperature (upper right) and relative humidity.

3. WIND SPEED AND DIRECTION

The standard wind speed and direction sensor set used in CODE is a ruggedized version of the standard reference anemometer manufactured by the the R.M. Young Co. and based on a three-cup rotor and vane design by G. Gill. The rotor (Model 6301) is 15 cm. in diameter and attached to a central steel shaft with a magnetic disc at the other end. Magnetized along a diameter, the disc produces two pole reversals with each rotation of the shaft. The inner assembly runs in stainless steel instrument ball bearings mounted in an aluminum housing which is threaded into a lower housing made of acetal plastic. This non-conducting material was used to prevent possible eddy-current damping effects between the rotating magnet and the housing. Although from later studies this damping effect appeared to be negligible, there is an unusual difference in the comparison studies which may be caused by it (see Chapter 8.) Figure 6 (right) is a section view of the anemometer; Figure 7 is an exploded view of the anemometer detail.

Rotor motion is sensed with a magneto-diode (Sony part number M0230A) cast in a polyurethane collar placed around the lower housing. With each half rotation of the anemometer cups, the magneto-diode signal initiates a compute cycle in the VAWR. During this cycle, the vector computer "reads" the compass heading and wind vane position and calculates and stores the magnetic East and North wind components. These vector components are summed for a specific interval, called the record interval, then permanently stored on magnetic tape as the vector average for that record. A 0.75 meter wind displacement causes one rotation of the anemometer above a threshold of about 0.2 m/s; the distance constant for the anemometer is 3.7 meters according to the R. M. Young specifications.

The wind vane (Model 6101) is a 78 cm. long aluminum shaft with a 23 cm. square thin aluminum vane on one end and counter-balance weight on the other (see Figure 6). The vane is mounted on a vertical bearing shaft with sealed stainless steel ball bearings. Attached directly to the vertical shaft is a seven-bit Gray-coded binary encoder. This encoder allows the position of the vane relative to the buoy to be measured optically with light-emitting diodes (LEDS) and photo-transistors (Figure 8). The wind vane orientation is read during the VAWR compute cycle and, when combined with the compass reading, is used to calculate the vector

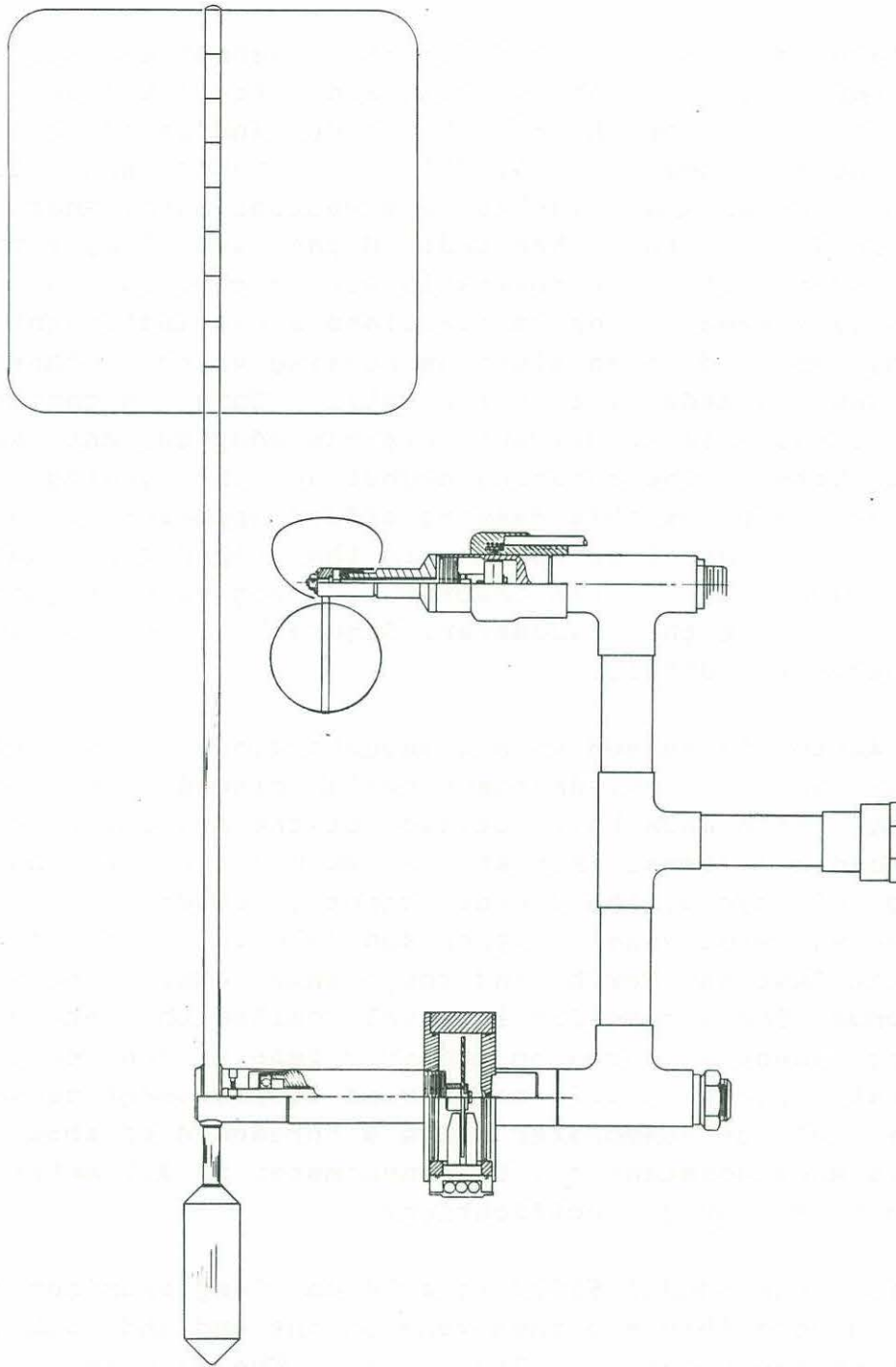


Figure 6. Section view of the Standard Gill VAWR cup anemometer and wind-vane assembly.

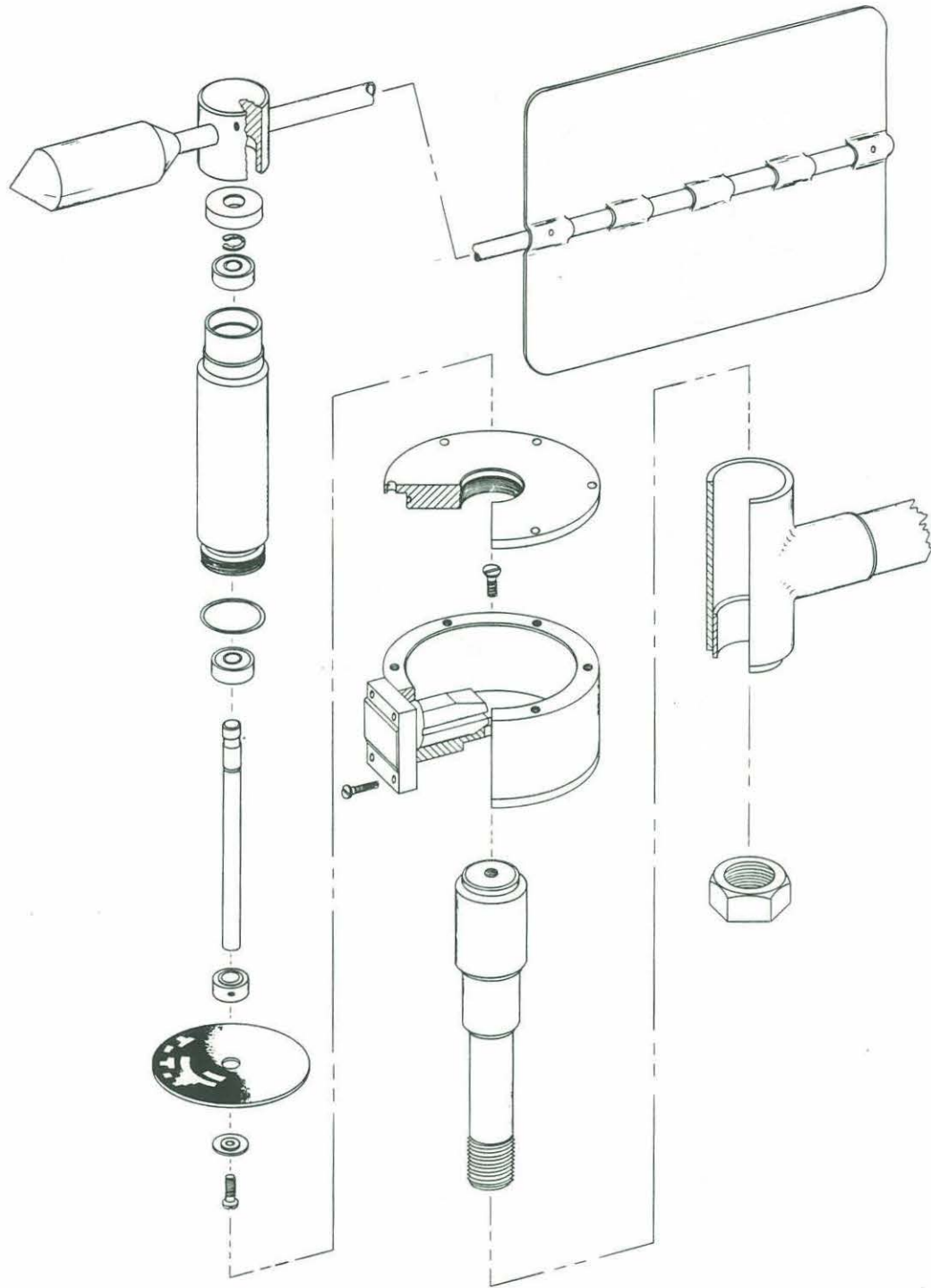


Figure 8. Exploded view of the wind-vane assembly.

components of the wind. This wind vane has a delay distance of about 1.2 meters according to the manufacturer.

As shown in the photos, Figures 2 and 3, the rotor and vane sensors are mounted at each end of a T-shaped bracket which in turn is mounted on the buoy tower, 3.5 meters above the water line. As the vane assembly measures the vane orientation relative to the mechanical assembly, the supporting structure must be aligned with the VAWR case and compass in order to provide accurate direction information. This alignment was done visually during the assembly of each VAWR on the toroidal buoy. After CODE-1, an integral VAWR was built for comparison with the standard sensor set and to simplify the assembly and alignment of the VAWR on the buoy. This integral design, now in common use at WHOI, is seen in Figures 3, 9 and 10. It is less tempting to sea birds, who sometimes are attracted to the larger vane and perch on it, fouling the wind data. In the integral VAWR, the wind vane is magnetically coupled to a vane follower installed inside the VAWR housing, and all alignments are done during the electronic shop assembly of the VAWR. The delay distance of the vane itself is 0.75 meters (calculated, following MacCready and Rex, 1964). The response characteristic is modified by the eddy-current damping in the vane follower which tends to smooth the high frequency flutter characteristic of the short vane. Results of the intercomparison of the two systems are discussed in more detail in Chapter 8. For a detailed discussion of cup and vane wind sensors, see Busch et al. (1980).

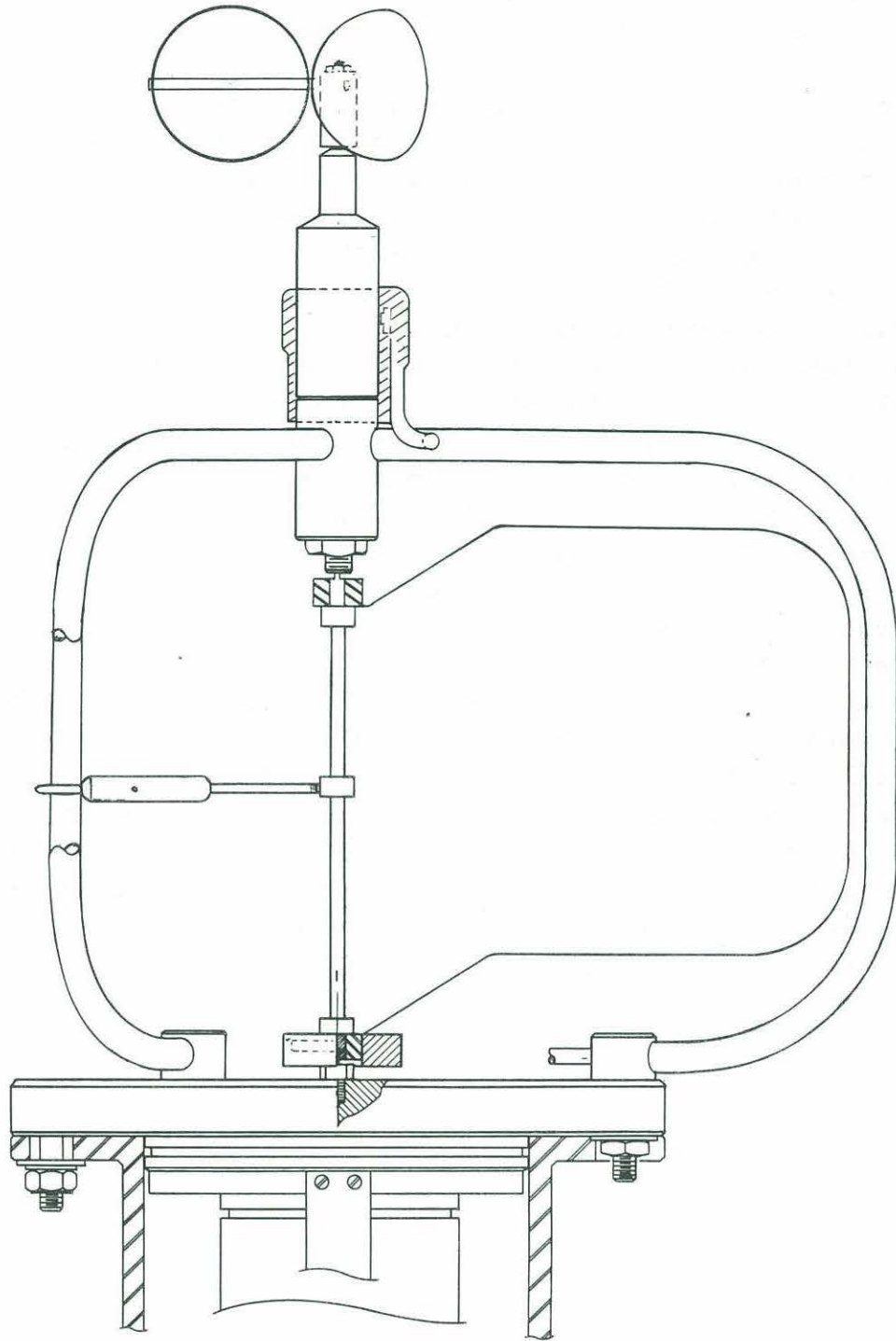


Figure 9. Assembly drawing of the integral cup and vane.

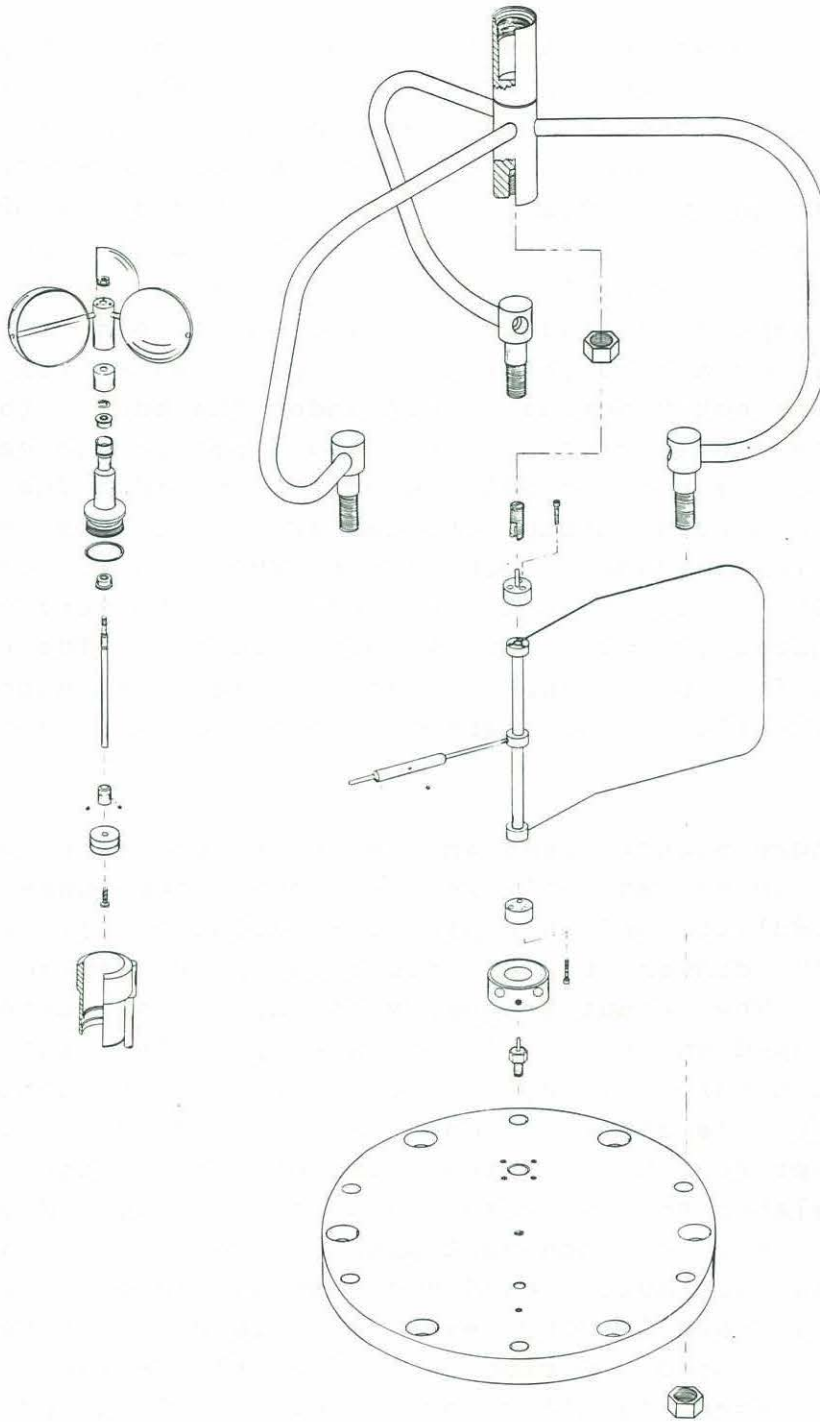


Figure 10. Exploded view of the Integral VAWR sensor set. ,

4. AIR AND WATER TEMPERATURE

Air and water temperature are measured with similar thermistor sensors and circuits in the VAWR. Air temperature is sensed at 3 meter height above the sea surface using a 5000 ohm at 25 ° C thermistor sensor accurate to 0.1 ° C (temperature-resistance characteristic known to 0.1 ° C.) The thermistor is protected in an acetal housing which is installed in a Thaller-type multiplate radiation shield, Figure 11, modeled after a design by G. Gill (1979). The sensor, protective housing and shield have a combined thermal time constant of about 150 seconds. Water temperature is measured at one meter nominal depth under the buoy with the sensor inserted in a pressure protected aluminum enclosure which is strapped to the stiff bridle under the toroid. The electrical cable runs through the center of the buoy and into the VAWR electronics package. This sensor, shown in Figure 12, is a 4000 ohm at 25 ° C calibrated thermistor with temperature-resistance characteristic known within 0.003° C. The thermal time constant for the assembly is about 7 seconds, short compared to the 110 second averaging interval used in the CODE instruments.

Each temperature sensor forms one leg of a resistance bridge circuit which drives an amplifier, a synchronous phase-sensitive detector/demodulator and an amplitude-modulated voltage-to-frequency (v/f) converter. A simplified block diagram is shown in Figure 13. The output frequency of the v/f converter is stored in an up-down counter and regularly shifted into a variable length buffer integrated circuit. The circuit components are time-shared or multiplexed through solid-state switches except for the individual sensors and bridge circuit components related to the sensor, and the nulling and balancing circuit components for each multiplex channel. Since as many as four variables were multiplexed over the 450-second (7.5 minute) record interval used in CODE, each variable was allotted 112.5 seconds. A 1.76 second period is used at the beginning of each variable measurement to allow for circuit settling and shifting data into the buffer from the previous measurement, leaving 110.74 seconds as the averaging time for each variable (exactly 110.7421875 sec.) The water temperature circuit operates with characteristic frequency output of ± 1165 Hertz with a temperature range of - 10 to 30 ° C. At 110.74 seconds averaging interval, the resolution or least count value is 0.00023 ° C. per data count.

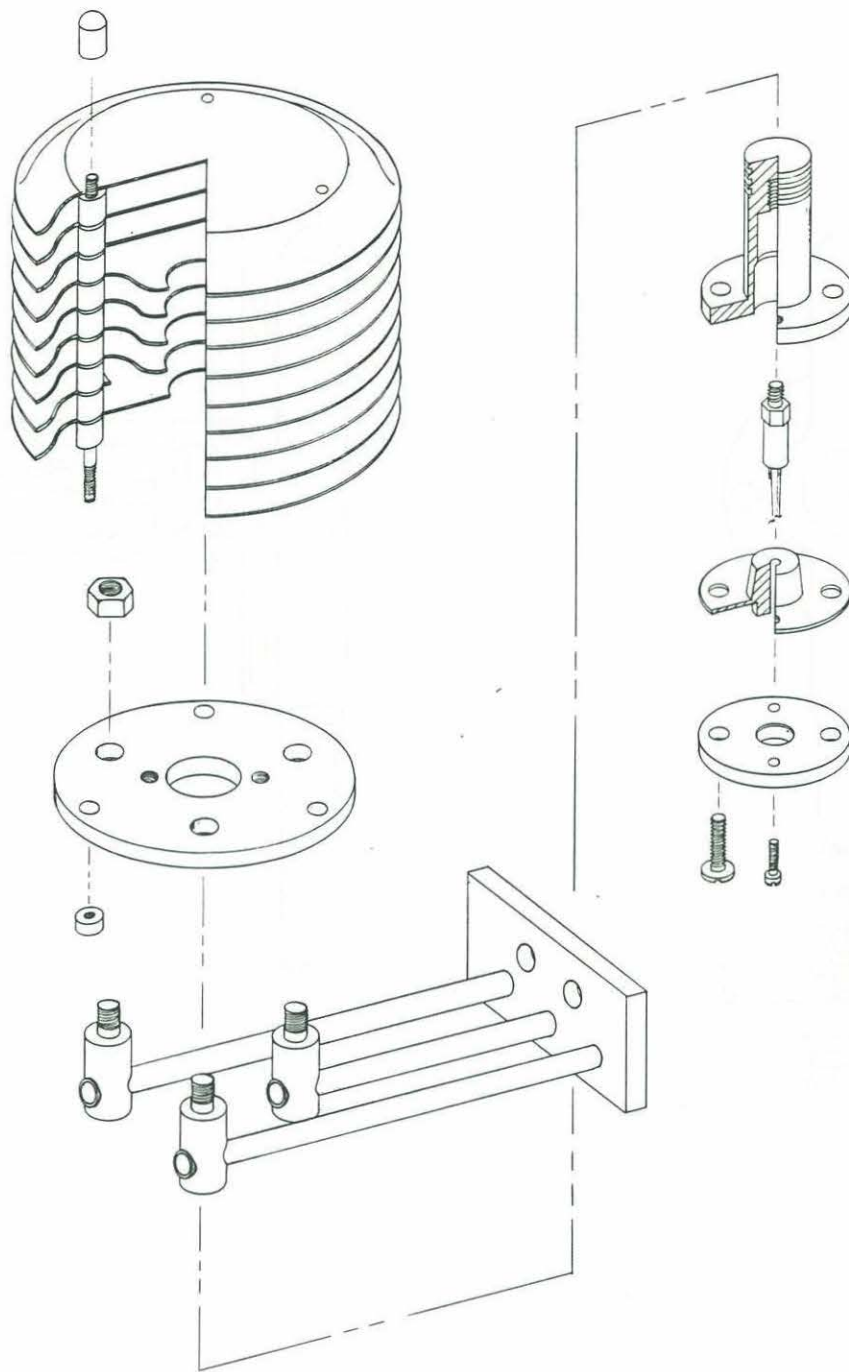


Figure 11. Exploded view of the Thaller-type multiplate radiation shield and air temperature sensor.

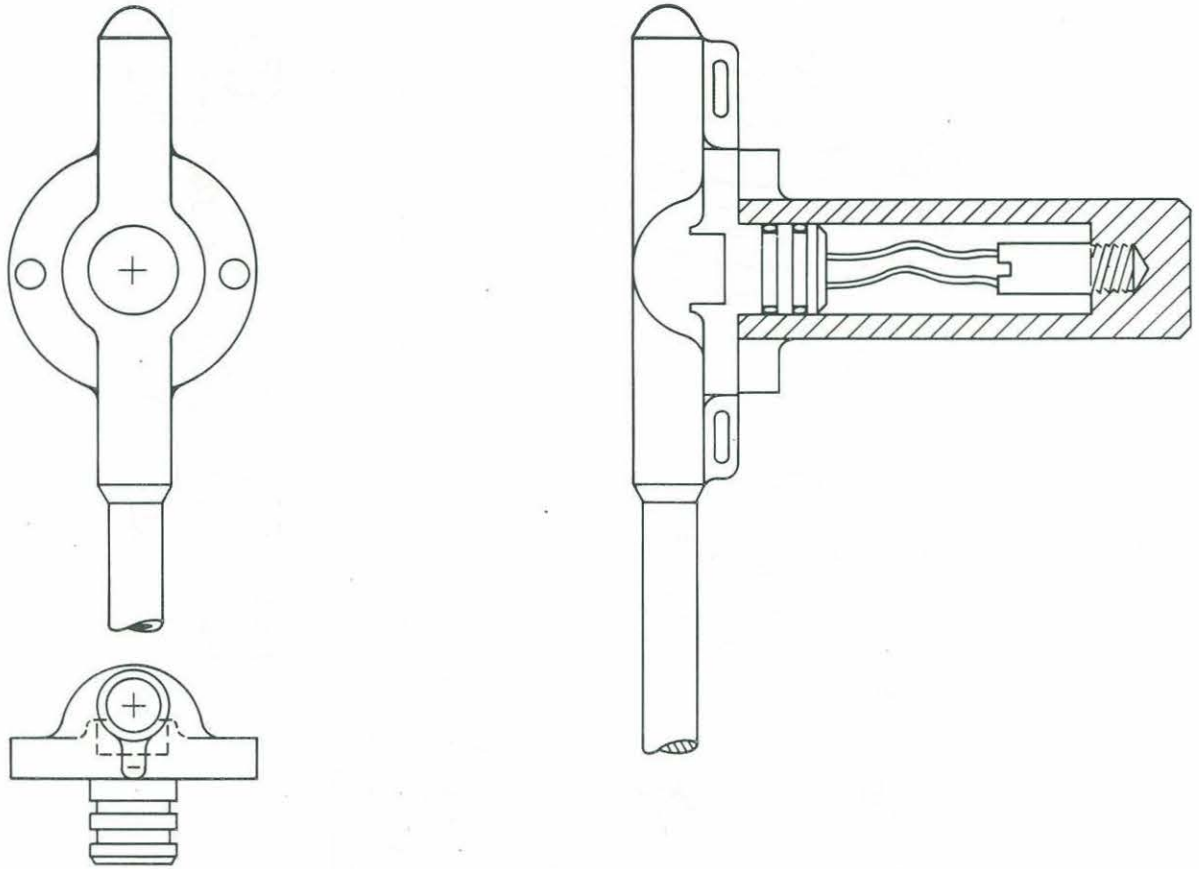


Figure 12. Section view of the water temperature sensor and its protective housing.

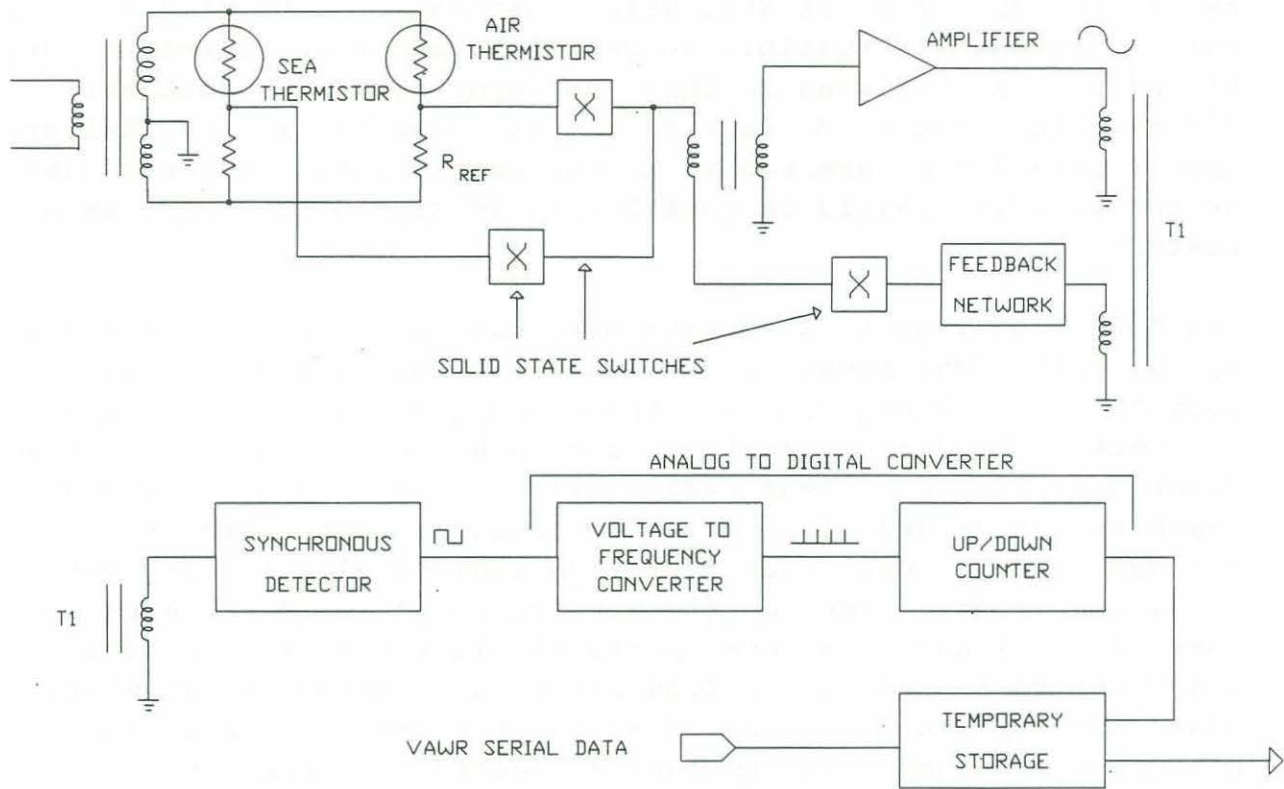


Figure 13. Simplified block diagram of the typical temperature channel of the multiplexed VAWR.

During CODE-1, two types of radiation shields were used for the air temperature sensors for both redundancy and intercomparison. These shields were later compared at a test tower on the roof of the Smith laboratory at WHOI with a naturally ventilated pivoted shield designed of multiple concentric plastic and aluminum tubes fitted with a wind vane so that the input port was constantly directed into the wind. As a result of these tests, the Thaller-type shield was determined to be the better shield and was used as the standard shield in CODE-2 (see Section 8 for comparison tests.)

The CODE-1 buoy-mounted shields were naturally ventilated designs by G. Gill. The first, a dome-shaped glass shield, purchased from the R. M. Young Company (their model No. 43103, Figure 14) consists of a 20 cm. diameter glass upper dome with inner surface painted white for maximum reflectivity. Glass is used because it tends to get washed clean of accumulated residue during rain. Two ABS plastic inner plates provide additional shielding yet allow free flow of ambient air between the shields and around the temperature sensor. A lower plate of black plastic reflects long-wave reflected energy from below and a second lower white plate with upturned lip was added for use over the water to protect the sensor from sunlight reflected from the ocean surface. This modification also shields the sensor from direct sunlight at very low angles.

The second radiation shield is a Thaller-type multiple plate design (Gill, 1979). Consisting of nine parallel aluminum plates 12.7 cm. (5 inches) in diameter, the stack is about 10 cm. high overall. The CODE shields were made at WHOI of aluminum, painted white, and are also shown in Figure 14. This multiplate design allows free flow of air but protects the sensor from direct or reflected sunlight from all angles. Similar plastic shields are now available from the R. M. Young Company. The C3 toroid buoy was designed with a large steering vane to maintain orientation of the meteorological sensors relative to the wind keeping the temperature sensors up-wind nearly all of the time. As a result the air heated by the metal tower did not pass over the temperature sensors. The other buoys were not so constructed; however it was later observed from airborne deposits left on the buoy that the radar reflector and other components on the buoy tower served as a vane to keep the temperature sensors upwind of the tower nearly all of the time.

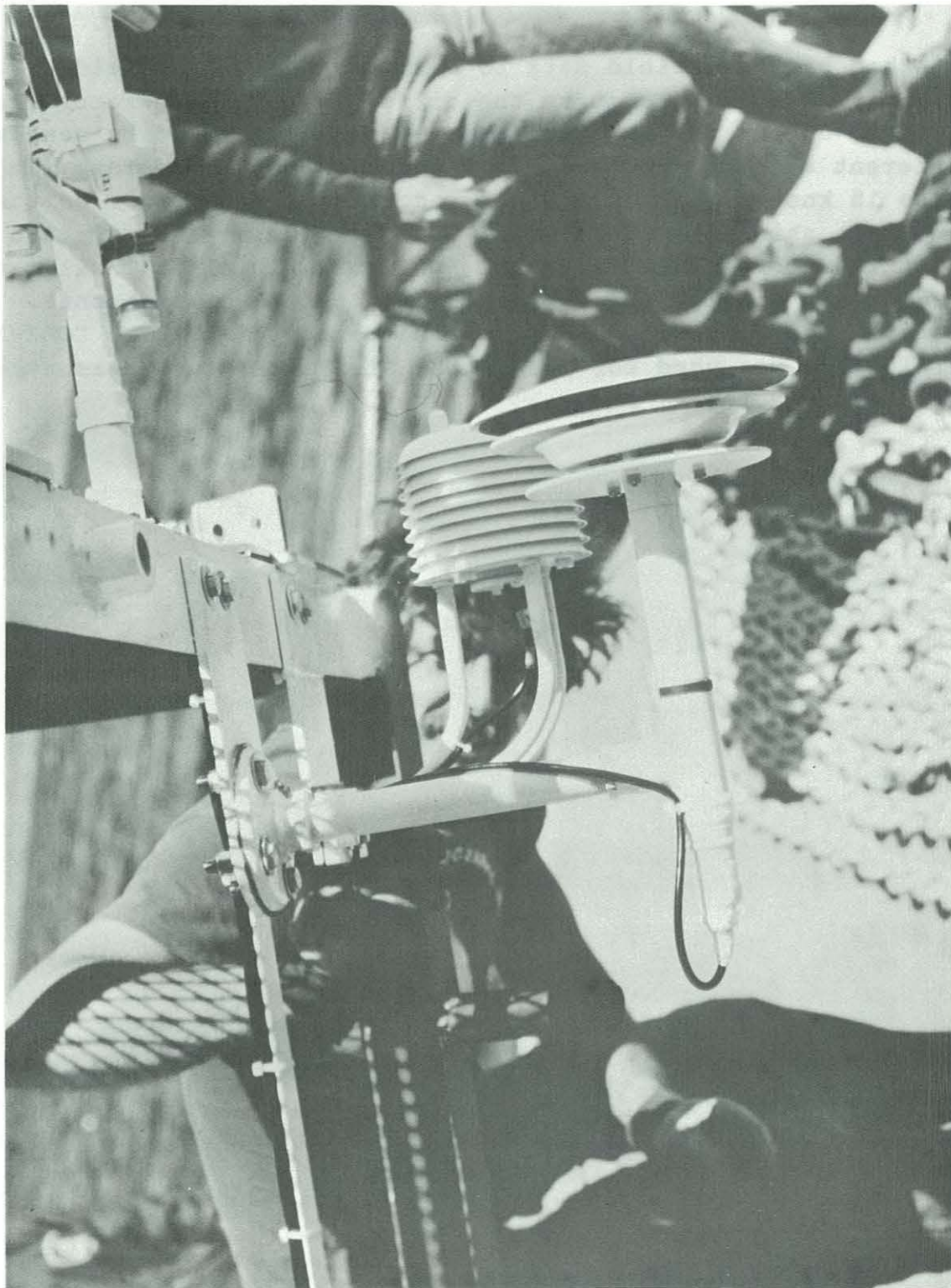


Figure 14. The dome-shaped radiation shield (right) and the Thaller shield mounted on the C-3 buoy tower for CODE-1.

A method of using field data to examine radiation shield effectiveness is to compare the differences in temperatures as measured during the day with that measured at night by sensors in different shields. On a typical sunny day with moderate winds of 10 to 15 knots, the temperature recorded by the sensor on the dome-type shield is about 0.4 ° C higher during the day than at night when compared to a sensor in a multiple plate Thaller-type shield (see Section 8 for a discussion of the comparisons). The multiple design was judged to be the better of the two CODE-1 shields and was used for all of the air temperature measurements during CODE-2.

5. INSOLATION

Insolation (incident solar radiation) measurements were made with pyranometers, hot-and-cold-junction thermopile transducers, which are sensitive to incident global solar radiation in the 0.35 to 2.5 micron range. Both an Eppley (The Eppley Laboratory, Inc., Newport, Rhode Island) model 8-48 and a Hy-Cal (Hy-Cal Engineering, Santa Fe Springs, California) model P-8405 pyranometer design were used in CODE. The Hy-Cal sensors exhibit an overall accuracy of about 5%, including temperature dependence, linearity and cosine response. The Eppley pyranometers have a specified accuracy of about 3% overall. In the Hy-Cal design, the sensor surfaces are sealed in a dry nitrogen atmosphere with a hemispherical lens. The Eppley sensor is also mounted under a hemispherical dome but is not sealed. Open to the atmosphere, it relies on a dessicant to prevent moisture condensation on the inside of the lens. They are both considered to be sufficiently rugged for use on a buoy.

These pyranometers are so designed that a blackened surface is exposed to the incident radiation and the resulting temperature rise compared to the temperature of an adjacent reference mass is measured with a thermopile, an array of thermocouple junctions. The low level DC output signal from the thermopile is amplified and used to modulate a voltage-to-frequency converter which provides input to a counter. The data are stored on magnetic tape at the end of each recording interval, comprising a measure of the average incident radiation for the interval.

Amplifier circuits for the two pyranometer models are identical and shown in block diagram in Figure 15. Adjustments were made in the amplifiers to account for the different sensitivities of individual transducers. The sensors are calibrated by the manufacturer and the output characteristic (slope of the linear curve) is supplied by the manufacturer.

The pyranometers were mounted on the buoy tower as shown in Figure 16, in a fixed position with minimum obstruction by other sensors. There was no attempt to gimbal the sensor; off-level errors were not measured and possibly caused additional error depending on the time of day, time of year, and the latitude (Katsaros and DeVault, 1986.) Two unpublished studies by R. Payne (personal communication) have estimated the mean tilts of a taut-moored toroidal buoy to be 10° or less for wind speeds less

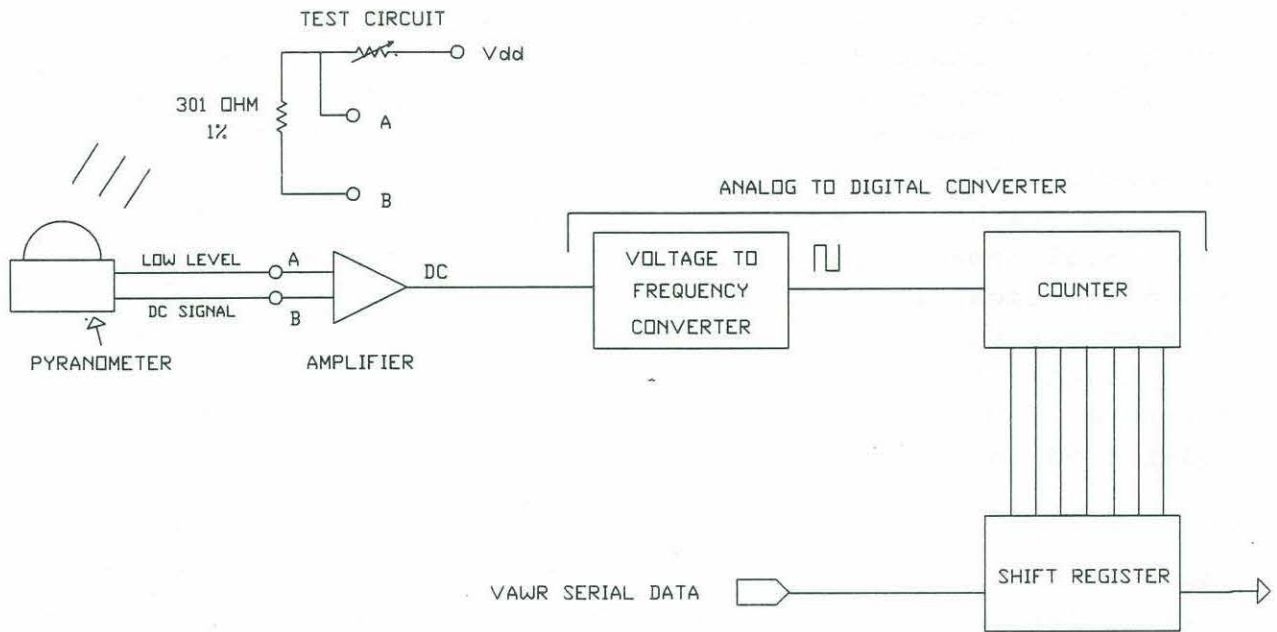


Figure 15. Simplified block diagram of the insolation circuits.

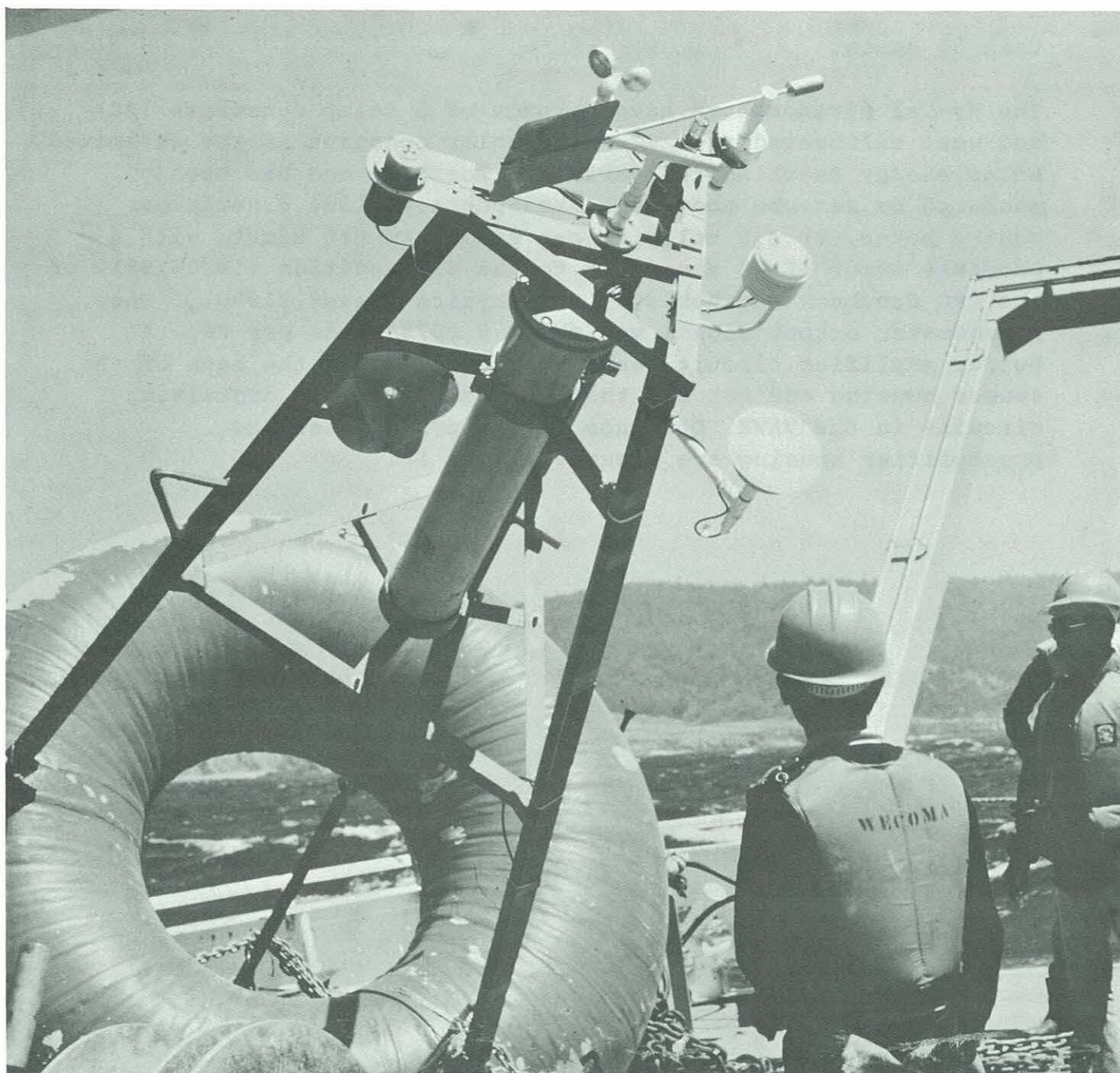


Figure 16. View of an Eppley pyranometer mounted on a CODE buoy tower (left.)

than 30 knots.

The Hy-Cal pyranometers have a range of 5 solar constants (SC) and were calibrated at 1 SC. One solar constant is the estimated solar energy reaching the earth's atmosphere and has been measured by sensors above the atmosphere at 1394.6 watts per square meter, or 2.0 calories per square cm per minute with a probable error of 2% according to the 61st edition (1980-1981) of the CRC Handbook of Chemistry and Physics (Weast, 1980). The pyranometer output signal was about 0.0075 volts per SC. A buffer amplifier circuit board was installed in the base of the sensor housing and matched the pyranometer to the digitizing circuits in the VAWR. Drawings of the pyranometer and preamplifier housing are Figures 17 and 18.

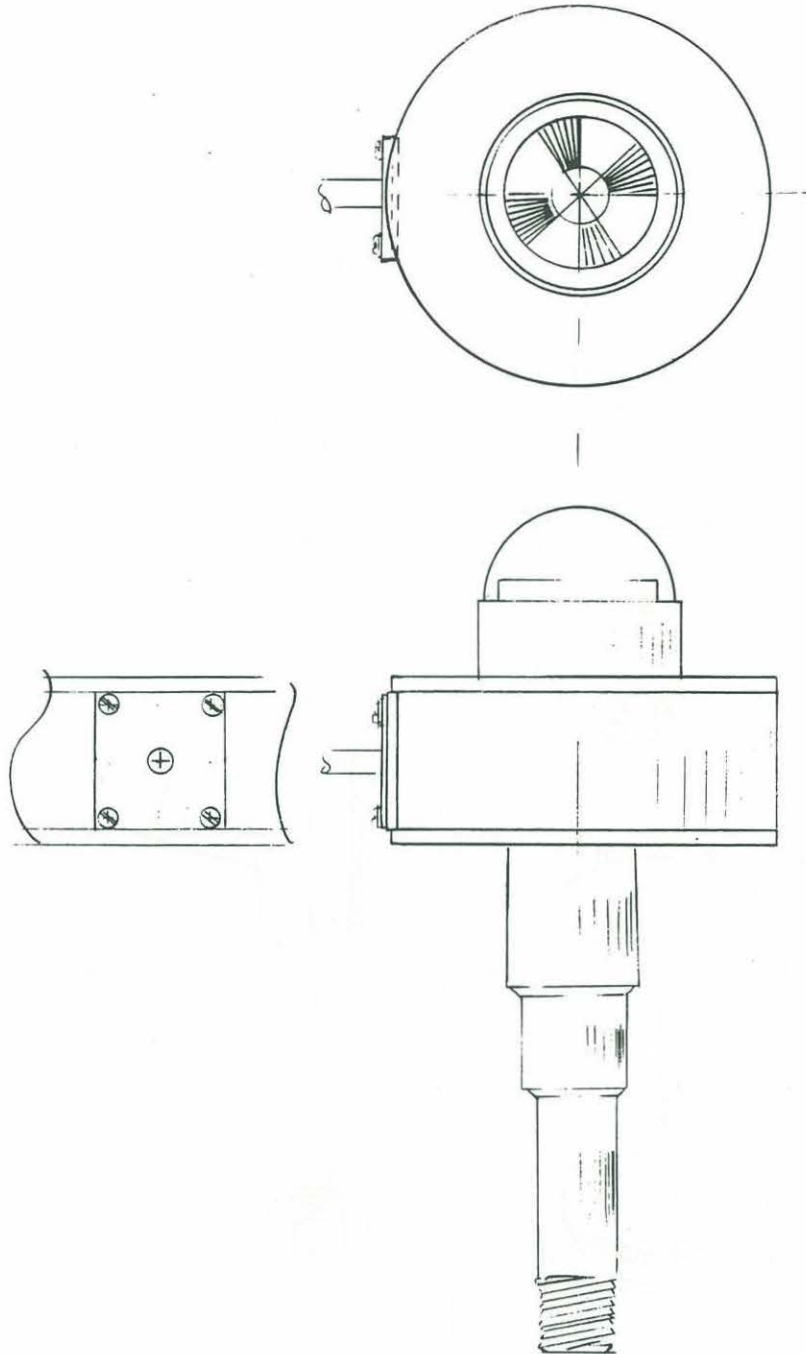


Figure 17. Assembly drawing of the Hy-Cal pyranometer and mount, with the amplifier housing.

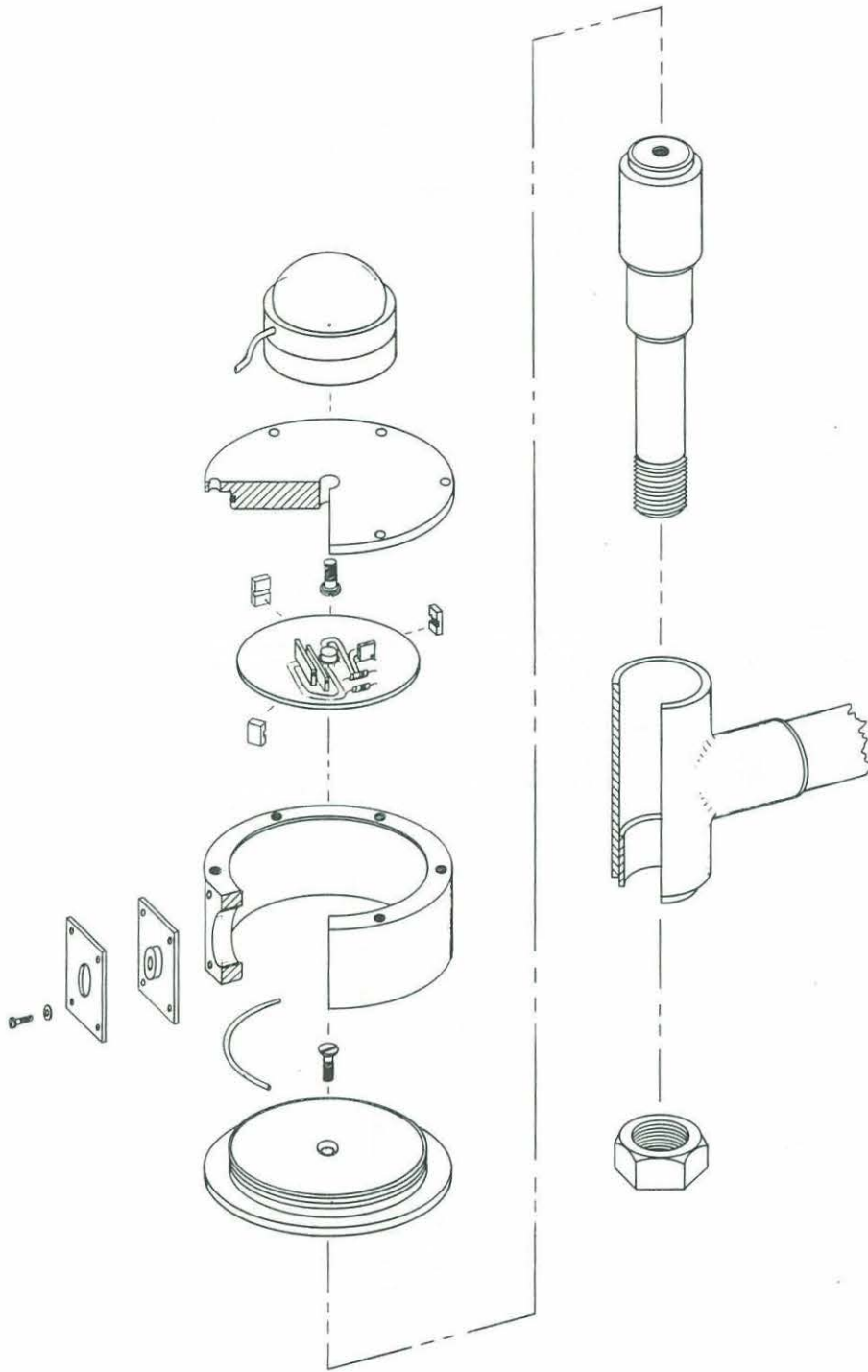


Figure 18. Exploded view of the insulation sensor assembly.

6. BAROMETRIC PRESSURE

Changes in atmospheric pressure are detected by a quartz crystal transducer (model 215-AS) manufactured by Paroscientific (Paroscientific, Inc., Redmond, Washington). Designed to operate over a range of 0 to 15 pounds per square inch absolute, the digiquartz sensor is the sensitive element in an oscillator circuit, the output frequency of which is stored and recorded as part of the VAWR serial data stream.

For use on a CODE buoy, the transducer housing includes a parallel-plate static pressure port based on a design by G. Gill (1976). This port shown in Figures 19 and 20 reduces the effects of wind to about 0.3 mbar for wind speeds less than 60 knots as shown in Figure 21 from Gill (1976).

To conserve total VAWR power drain, the transducer power was switched on for a brief time, then off again. During the "on time", following a brief settling interval, data were stored during a 2.6 second measuring period. Figure 22 is a block diagram of the pressure circuitry. The range of the pressure system was zero to 1240 millibars (mbar) and the resolution was 0.1 mbar.

Calibrations were done by the manufacturer or at a WHOI test facility and the accuracy is certified by the manufacturer to within ± 0.015 percent, resulting in sensor accuracy within 0.15 mbar at 1000 mbar.

Recent (1986) studies have revealed a serious instability problem with the sensor type used in CODE (Model 215-AS). According to Donald Busse, Paroscientific Vice President, the vacuum chamber of this sensor was sealed with epoxy, and exposure to a humid environment may have accelerated the diffusion of water molecules through the epoxy. The result has been a temporal drift of about 0.14% (.15 mbar) per year compared to the manufacturer's specification of 0.017% (0.017 mbar) and a thermal sensitivity of 0.03% (.31 mbar) per degree C compared to the advertised specification of .0047% per degree.

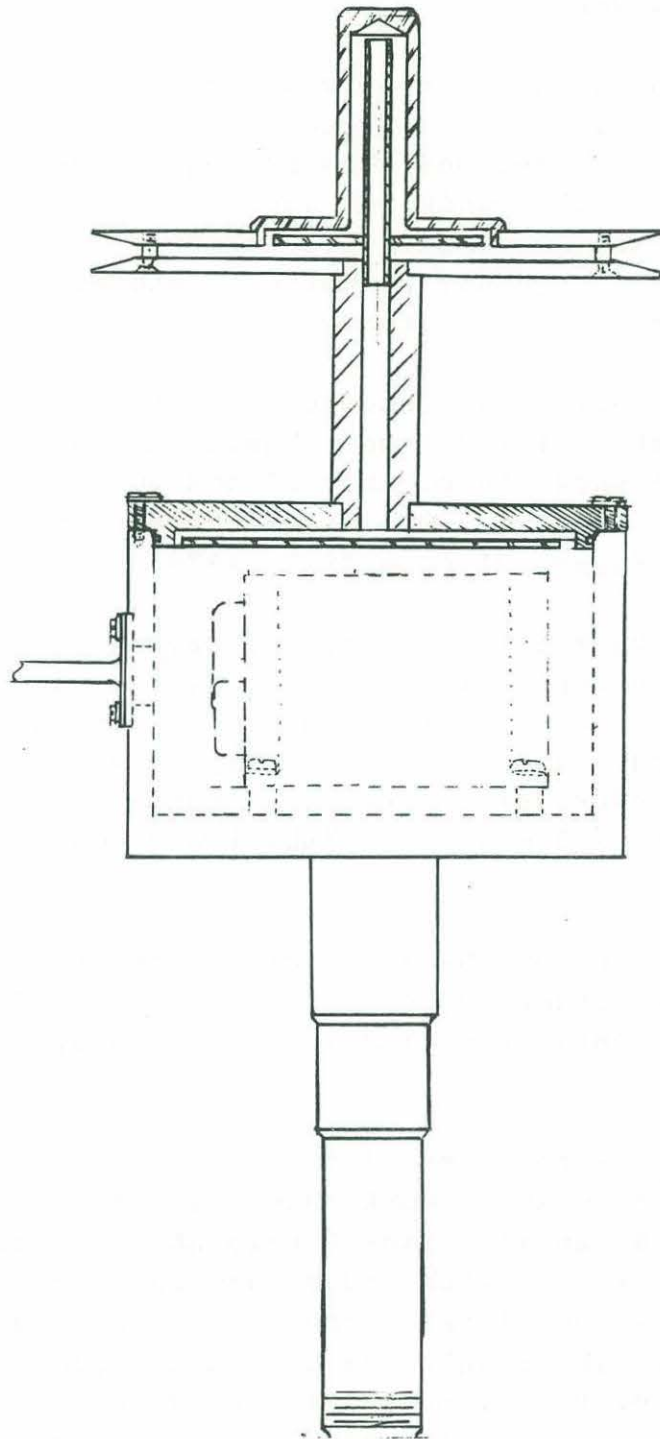


Figure 19. Section view of the parallel-plate port for barometric pressure measurements from a buoy. After a design by Gerry Gill (Gill, 1976).

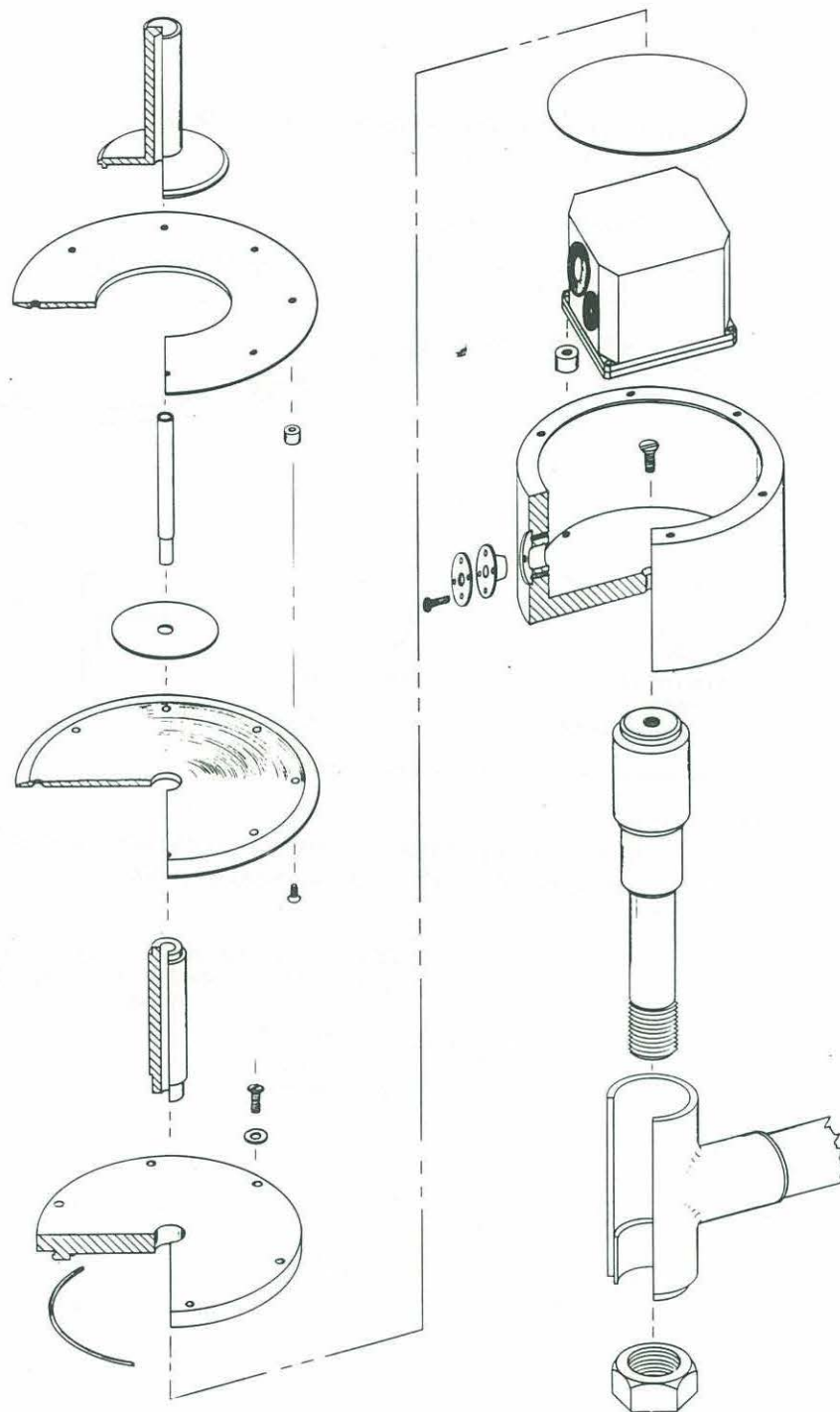


Figure 20. Exploded view of the parallel-plate port and sensor housing for barometric pressure measurements.

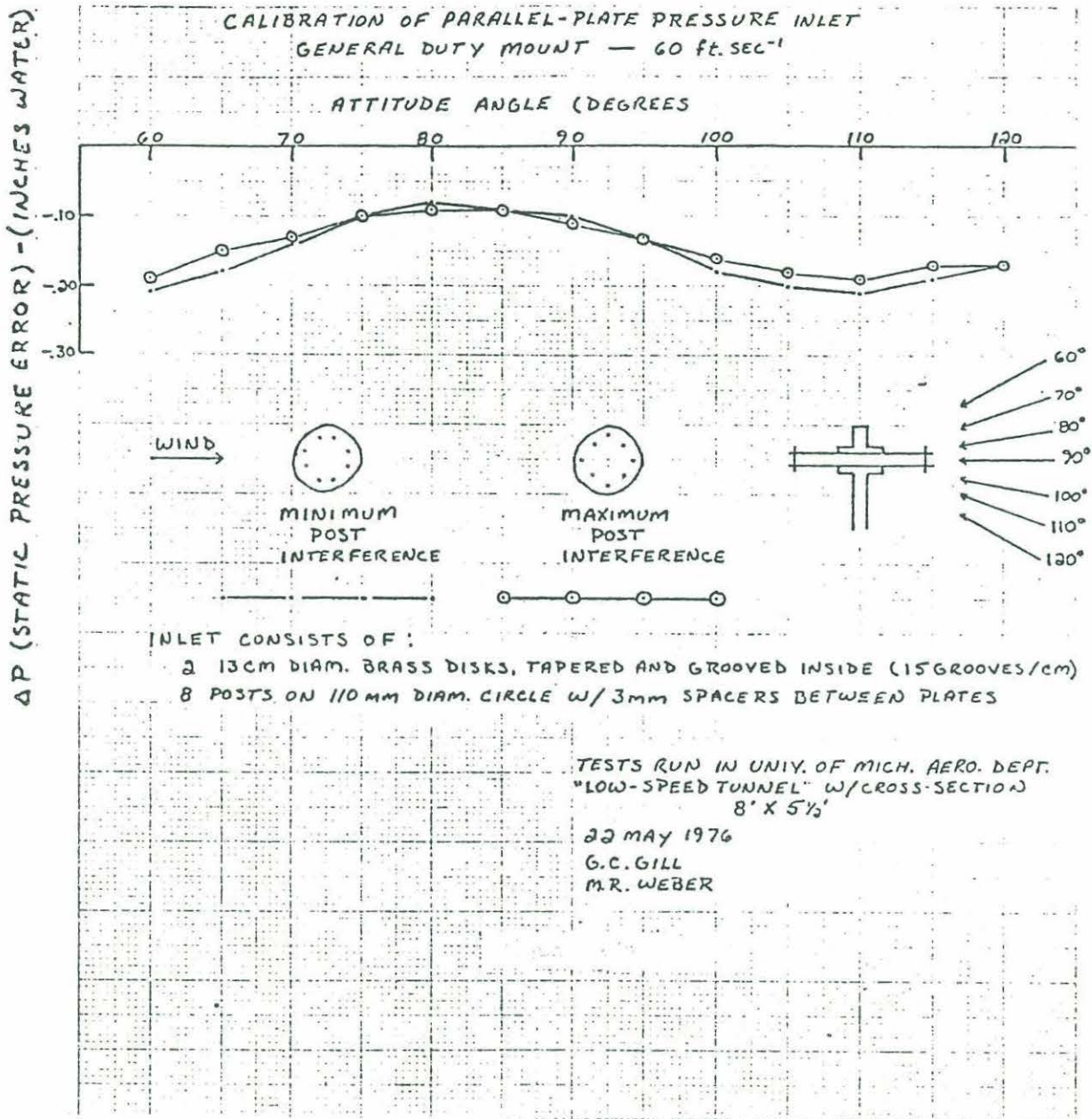


Figure 21. Static pressure error of pressure measurements made with the parallel-plate port of Figures 19 and 20. The plot depicts how the error varies with vertical orientation of the port to the direction of the wind. Pressure difference of 0.1 inch of water equals 0.25 mbars; typical buoy inclination is estimated to be less than 10°. This figure is reproduced from Gill, 1976.

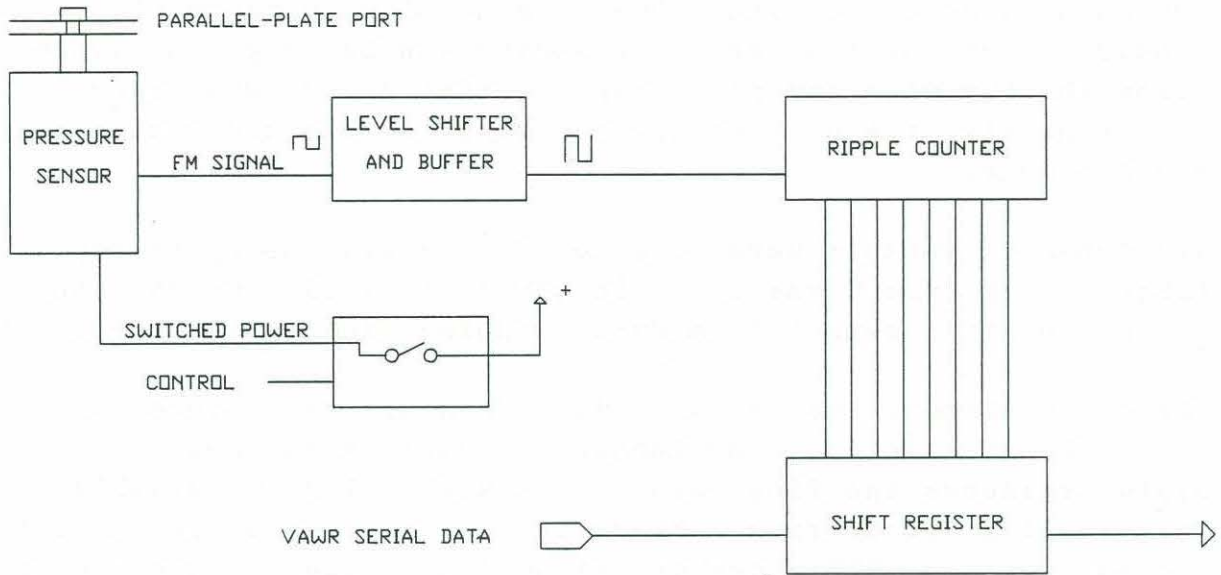


Figure 22. Simplified block diagram of the barometric pressure circuits in the VAWR.

7. RELATIVE HUMIDITY

Attempts were made to measure and record relative humidity from two stations during the CODE-2 small scale array. Humidity is an elusive measurement to make from remote, unattended self-recording stations at sea. Due to scheduling constraints, consideration for the choice of sensor was based primarily on compatibility with and power capabilities of the wind recorder. Unfortunately, the data return was very low and the data quality questionable.

Two types of sensors were considered; one was the hygroscopic fiber sensor from Texas Electric (Model TA 2013) and the other a cellulose strip sensor from Hy-Cal Engineering (Model HS-3552-B).

The fiber element reacts to changes in humidity in much the same way as human hair, getting longer as humidity increases. The system measures the fiber elongation with a linear variable differential transformer. Electrically, the system is ideal for the multiplexed VAWR; however, without modification the sensor assembly is inherently sensitive to vertical accelerations of a surface buoy platform.

The Hy-Cal sensor consists of a cellulose crystallite strip which reacts to changes in humidity much the same as a bimetal strip reacts to changes in temperature. Strain gauges are attached to a metal beam which in turn is secured to the humidity sensitive strip and forms a resistance bridge circuit compatible with the VAWR data input circuits (see Figure 23.) The Hy-Cal unit seemed rugged and suitable for use on the buoy and similar sensors had been used in the past (Payne, 1974).

VAWRs at stations C3 and C5 were modified for relative humidity measurements with the Hy-Cal sensors. The sensor (Figure 24) installed on the C5 VAWR developed a problem and returned no data. The C3 sensor worked throughout the term of deployment and agreed with independent measurements on the site to within about 5%. The sensor was very susceptible to contamination by salt in the ocean atmosphere. The data were recorded as one of four multiplexed variables and decoded using calibration information supplied by the vendor.

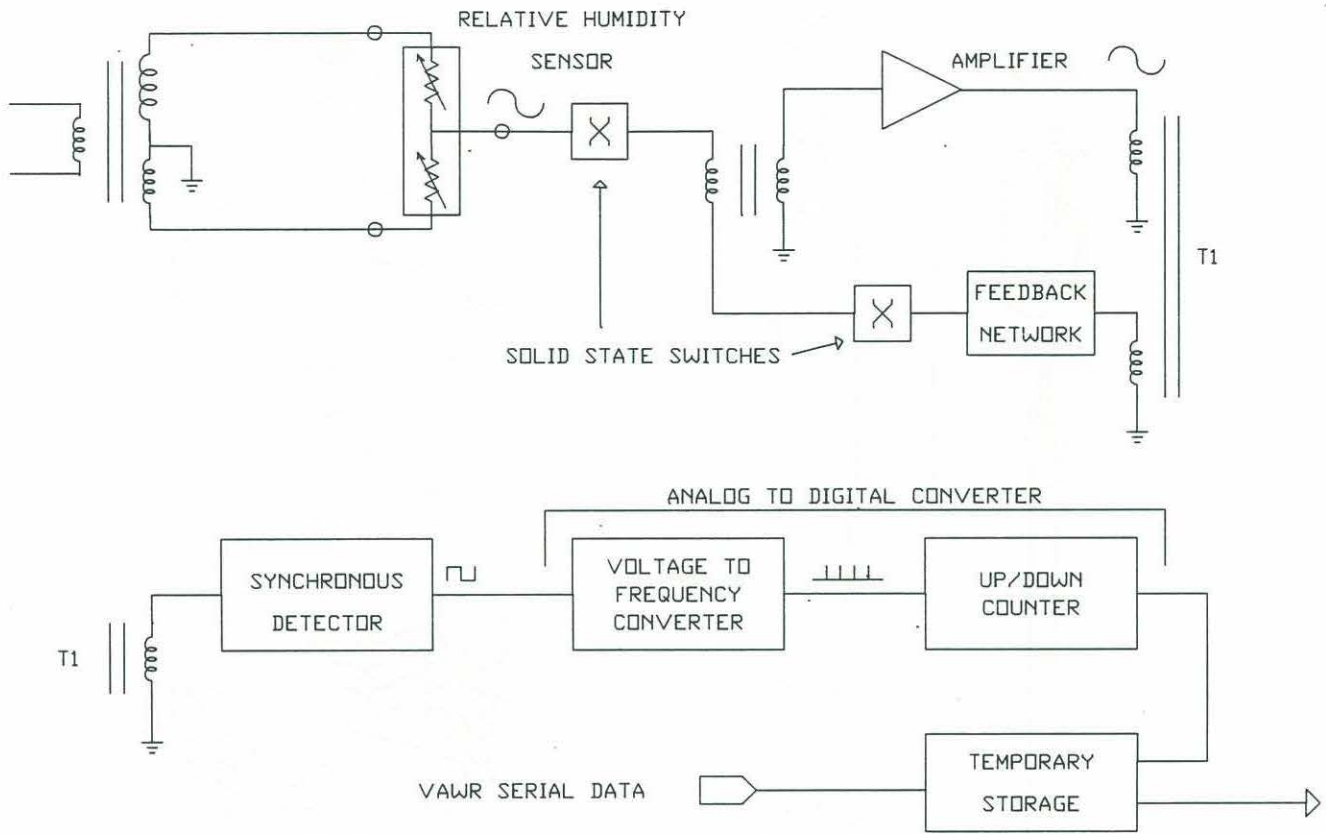


Figure 23. Simplified block diagram of the relative humidity circuits in the VAWR.

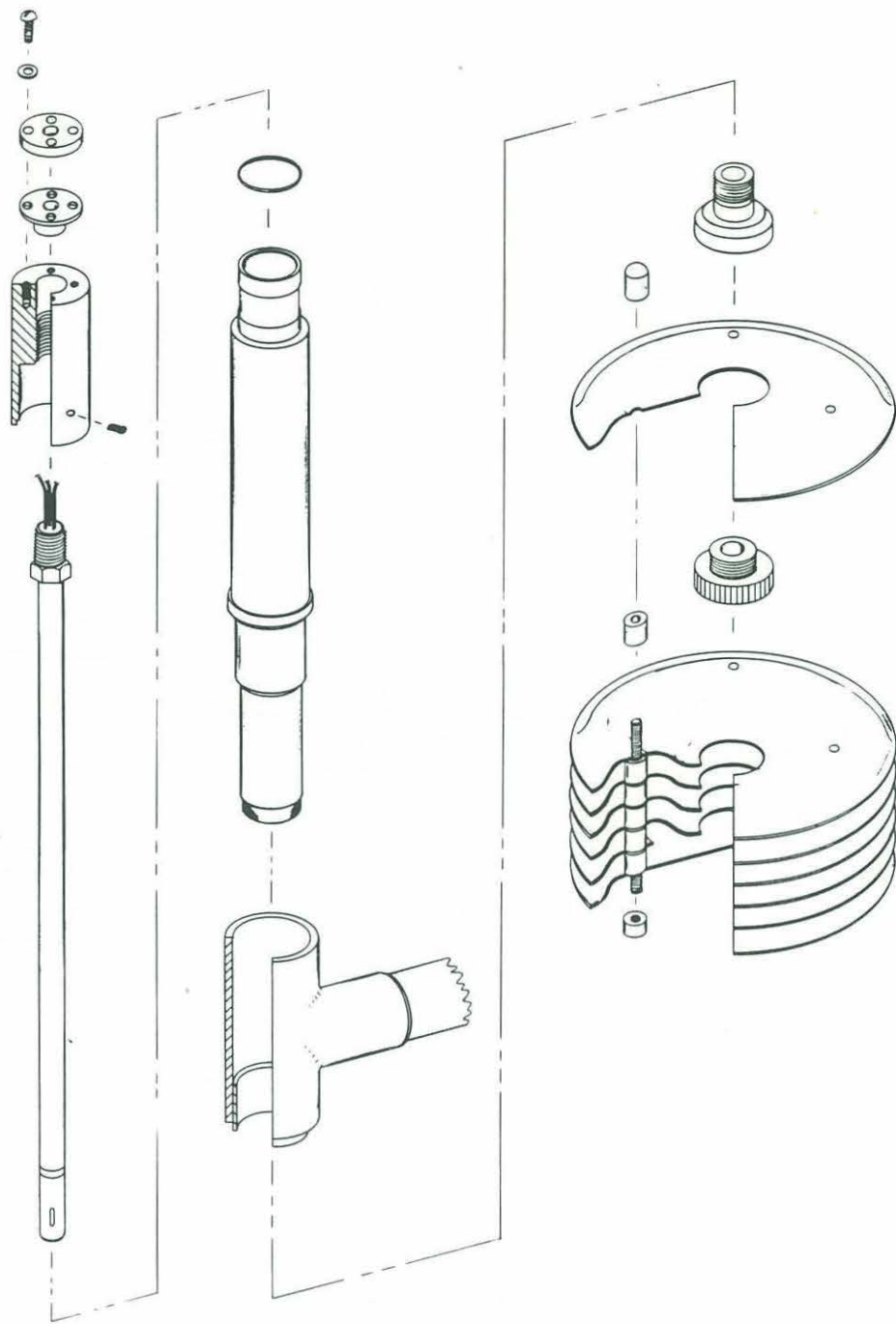


Figure 24. Exploded view of the HyCal relative humidity sensor, mounting brackets and radiation shield.

8. INTERCOMPARISONS

Intercomparisons of some meteorological sensors were conducted during CODE. Radiation shields for the air temperature sensors were compared with each other, two types of pyranometers were intercompared, and wind speed and direction data from three types of wind sensors used during the field work have been analysed. Results of the intercomparisons are described here.

8.1 *Field intercomparisons of different wind sensors.*

As C3 was the most crucial mid-shelf mooring site, two separate wind recorders were deployed on this toroid in CODE-1 and CODE-2 for both wind measurement redundancy and engineering comparisons. The basic wind sensor set used on the CODE Standard VAWR was the R. M. Young (Model 6001) utility wind sensor set, modified as described in Section 3. It was designed by Gerry Gill, is here called the Gill wind sensor set, and was the common reference for the intercomparisons. A Standard VAWR with Gill sensors and a then-new EG&G VMCM modified to be a vector measuring wind recorder (VMWR) were deployed in CODE-1 and a Standard VAWR and an Integral VAWR were deployed in CODE-2. All four wind recorders worked for at least part of the deployment period, and a comparison of the wind measurements follows.

Basic statistics for the CODE-1 and CODE-2 wind sensor comparisons are given in Table II. After initial editing, the basic wind time series were vector-averaged into 1-hour time series and rotated into a common coordinate system with the orientation of the positive cross-shelf component (designated U) pointing towards 47° T (True) and the positive along-shelf component (V) pointing towards 317° T. Statistics of the cross-shelf and along-shelf component, speed (S) and direction (θ) difference time series based on the hourly vector-averaged time series are designated by dU, dV, dS, and d θ , respectively. The subscripts a, m, and i identify the Standard VAWR, the VMWR and the Integral VAWR, respectively. See Section 3 of this report for a detailed description of the wind recorders.

8.1.1 *VAWR and VMWR intercomparison in CODE-1.*

In CODE-1, an EG&G VMCM was modified with thin (1/16 inch thick), light-weight delrin propeller blades for use as a wind recorder and is called a VMWR (Vector Measuring Wind Recorder). The

TABLE II

Wind sensor intercomparison statistics
(See text for definition of the variables)

Experiment	Variable	Mean (m/s)	Std. Dev.	Maximum (m/s)	Minimum (m/s)	
CODE-1	U_a	0.23	1.17	4.04	-3.19	
	U_m	0.25	1.46	5.19	-3.17	
	dV	0.03	0.43	1.85	-0.80	
	V_a	-8.86	3.88	2.81	-15.30	
	V_m	-9.41	4.23	2.54	-14.93	
	dV	-0.56	0.60	1.40	-1.94	
	S_a	9.02	3.67	15.36	0.28	
	S_m	9.60	4.06	15.14	0.04	
	dS	0.58	0.60	1.94	-0.97	
	d θ	-0.47	3.54	21.70	-45.80	
	Complex Correlation (0.998, 0.36°)					
	CODE-2	U_a	0.58	1.17	4.70	-2.62
		U_m	0.63	1.17	4.78	-2.50
		dV	0.04	0.08	0.35	-0.32
		V_a	-8.86	3.88	2.81	-15.72
V_m		-5.86	5.60	7.82	-15.60	
dV		-0.02	0.08	0.33	-0.36	
S_a		7.13	4.14	15.88	0.13	
S_m		7.10	4.13	15.75	0.04	
dS		-0.03	0.07	0.33	-0.32	
d θ		-0.53	1.57	16.71	-20.89	
Complex Correlation (0.992, 0.47°)						

propellers were changed to reduce the weight and angular moment of inertia and improve (i.e. shorten) the distance constant. The instrument was deployed on a steered buoy with the sensor set aligned approximately 45° into the wind as shown in Figure 2. Both instruments functioned correctly for about the first month of deployment before the bearings failed in the VMWR. Thus the VAWR versus VMWR intercomparison was made during the 28 day period between April 12 and May 10, 1981. To test for possible compass offset and sensor alignment errors, the complex correlation coefficient was computed between the two wind time series (Mooers, 1976).

As the VAWR and the VMWR wind velocities are highly correlated and always nearly parallel, scatter plots of the VMWR speed, and speed and direction difference versus VAWR speed shown in Figures 25, 26, and 27 illustrate the general response of the two instruments in this experiment. To construct these scatter plots, the hourly data shown in the middle panels have been sorted by VAWR wind speed into 2 m/s wide bins, and the mean and the standard deviations of the data points within each bin computed and plotted in the top panels. The number of data points within each bin is shown in histograms in the bottom panel. Both the original data and the bin-averaged wind speed data clearly show that the VMWR wind speed, S_m , is generally less than the VAWR speed, S_a , at wind speeds less than about 6 m/s. At intermediate wind speeds between about 6 and 14 m/s, the VMWR speeds typically exceed the VAWR speeds by as much as 1.5 m/s or up to 12 %.

The VMWR and Gill sensors again agree at the higher wind speeds, and the cause is not obvious. One can speculate about a reduction in sensitivity due to an increase in bearing friction at high speeds as a result of the higher axial load, a reasonable theory since the bearings did fail prematurely. This hypothesis is somewhat verified by the direction difference plot, Figure 27. If the wind load on one of the propellers differs from the other and the bearing friction reduces that propeller sensitivity, then the direction, which is derived from the components from both propellers, would be in error at high speeds. A plot of the Gill VAWR and the VMWR wind speed and direction comparison is given in Figure 28. Shown here are a time series of the cup speed, the difference in direction between the two wind vectors, and the difference speed for the two sensors. Except for spikes when the direction is rapidly changing and the instrument clocks are

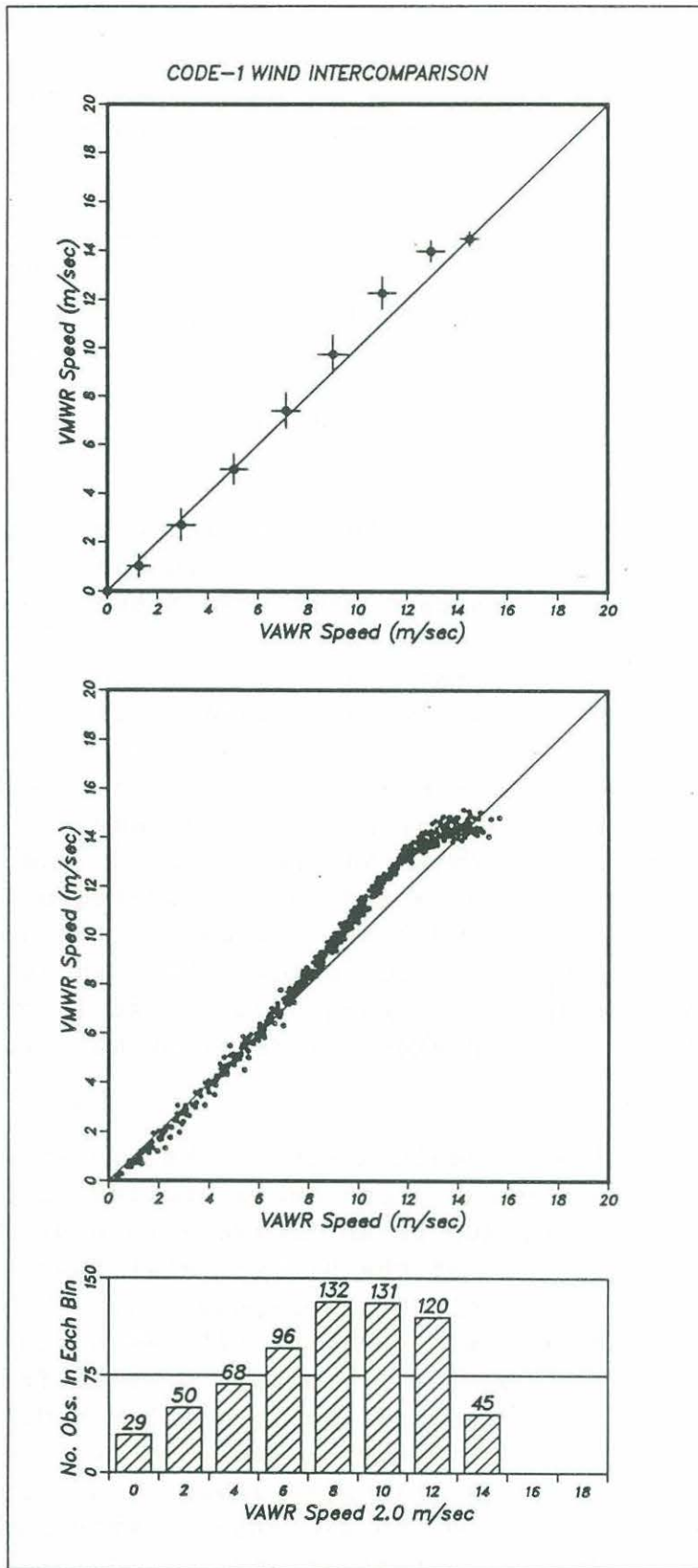


Figure 25. Histogram and scatter plots of the wind speed measurements made with the VAWR and VMWR in CODE-1.

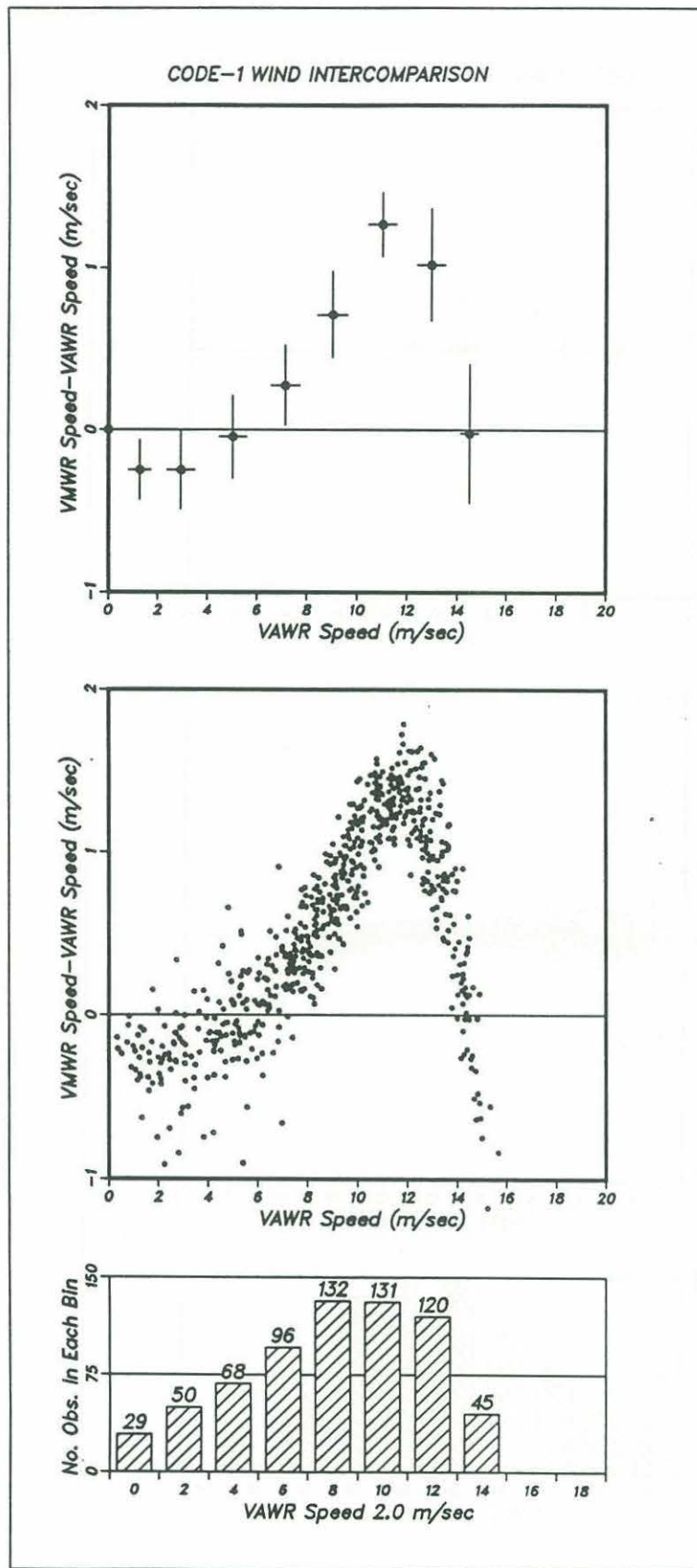


Figure 26. Histogram and scatter plots of the VAWR and VMWR speed difference versus wind speed in CODE-1.

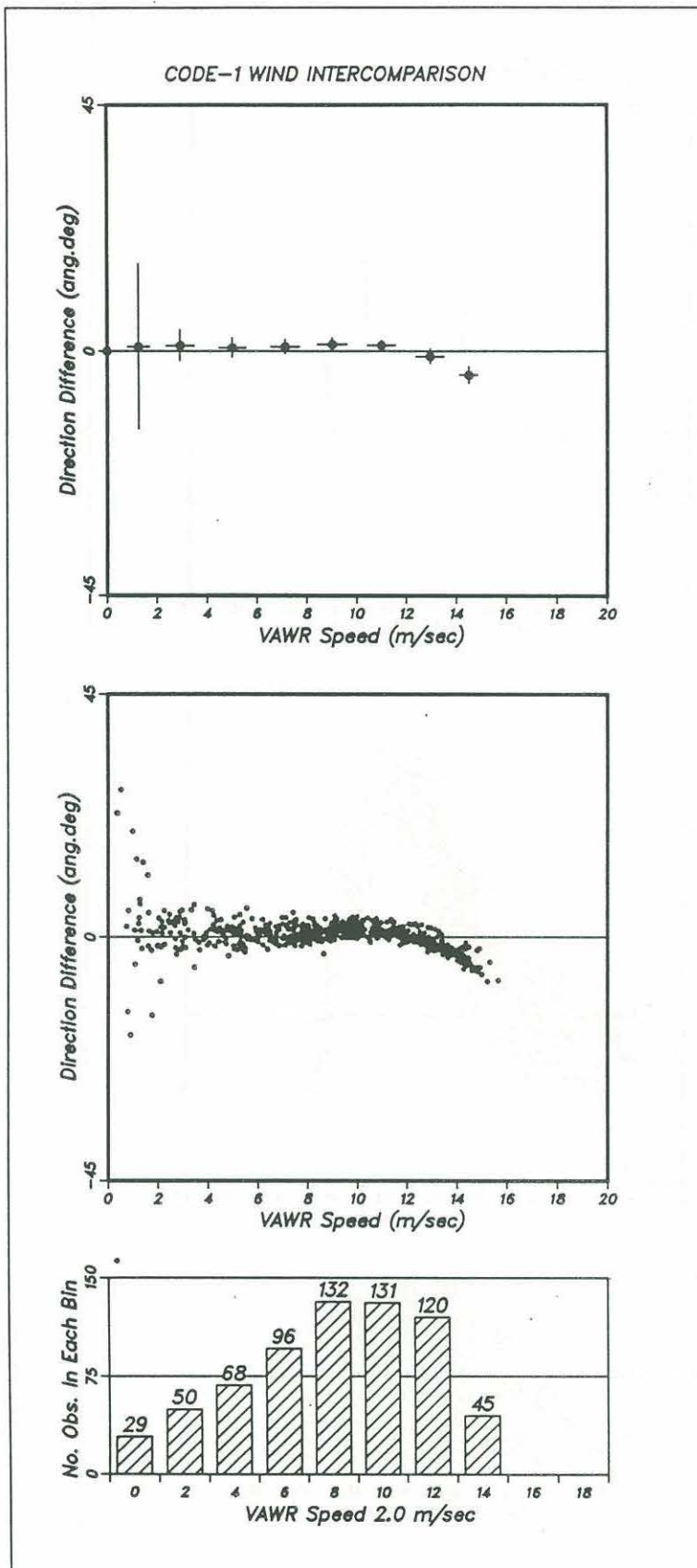


Figure 27. Histogram and scatter plots of the direction differences versus wind speed for the VAWR and VMWR in CODE-1.

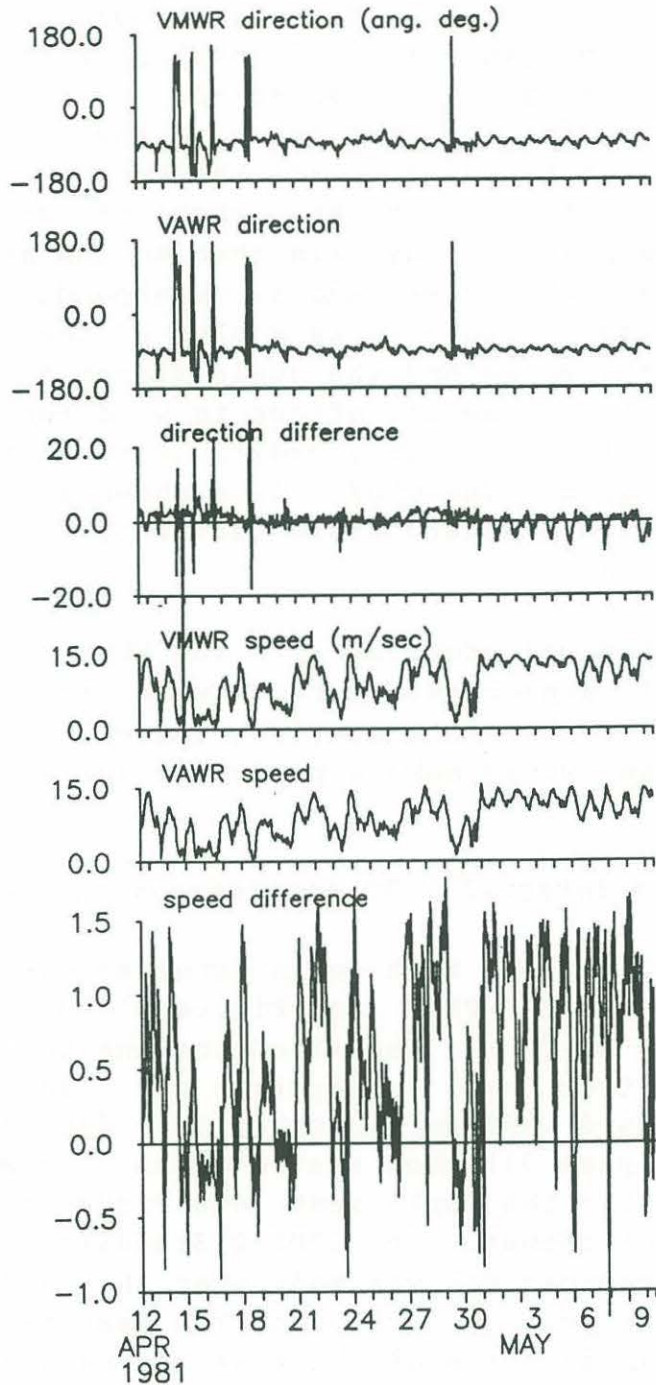


Figure 28. Time series of speed and direction (rotated into local geographic coordinates as defined in the text) for the VAWR with Gill wind sensor set, the modified VMWR, and the differences in the signals as measured by the two systems in CODE 1.

slightly out of synchronism, the directions agree within about 4° . The speeds fall within a ± 1 m/s envelope with the VMWR apparently overestimating the higher speeds. Data from subsequent tests suggests that the cause of the error may be the result of changing the propeller blade thickness. The 1/16 thick blades used in the VMWR have a higher (about 6%) along-axis scale factor for winds parallel to the axis than do the standard VMCM propellers with 1/8 inch blades, and a corresponding non-cosinusoidal response. Figure 29 is a plot of the relationship between the blade thickness and the scale factor for the VMCM propeller. Payne (1981) saw the effect in wind tunnel tests but the cause was then attributed to a modification in the hub design which was being studied. The CODE-1 data shown in this report was computed using the standard scale factor of 2.67 revolutions per meter of wind run.

Because of the mechanical problems with the VMWR and the good result with the Gill sensor set, further work with the VMWR was not pursued, even though this comparison suggests that the VMWR, if properly modified, would make a perfectly suitable wind recorder.

8.1.2. *Standard and Integral VAWR comparisons in CODE-2.*

In CODE-2, a redundant VAWR with an integral sensor set was deployed with the Standard VAWR (see Figure 3) on the central meteorological buoy at C3 and is called the Integral VAWR. A comparison of data from these two systems was also made. The data from the standard VAWR were rotated 14.5 degrees (Limeburner, 1985, page 31) when system blocked vane direction tests before and after the deployment (see Figure 3) showed a consistent alignment offset. The CODE-2 Standard VAWR versus Integral VAWR intercomparison was made over the 76 day period between April 15 and June 30, 1982, and the results presented here are based on an analysis of the rotated one-hour vector-averaged time series. The computed correlation coefficient was 0.998, with a phase angle of 0.36° , indicating that both vector time series were very highly correlated and the stronger wind vectors were on average rotated by only 0.36° with respect to each other. Since this small mean rotation was well within the uncertainty of the compasses, no angular correction was made to either wind time series. Other statistics are listed in Table II.

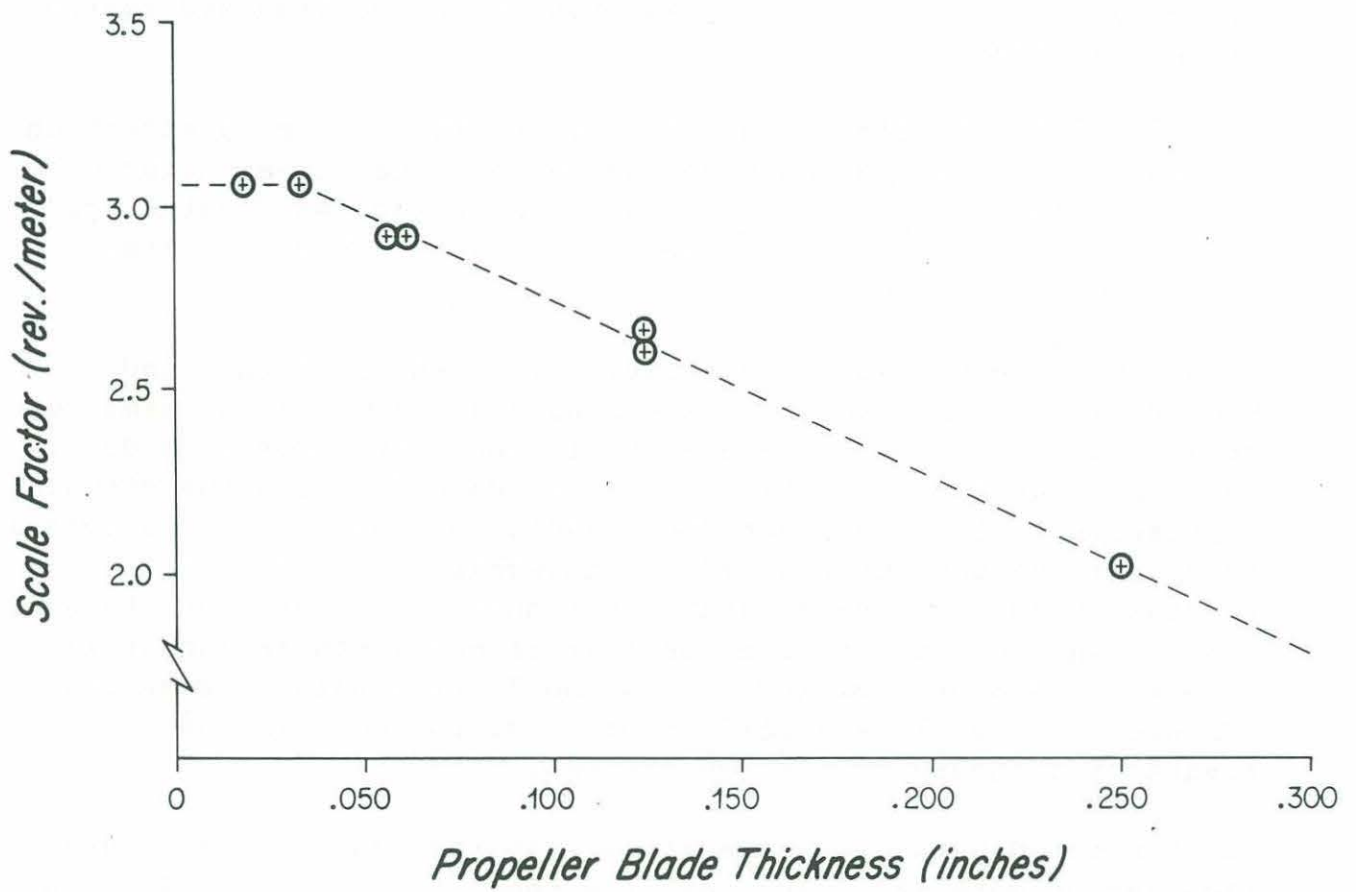


Figure 29. Variation of the scale factor with blade thickness for the VMCM or VMWR propeller.

Plots of the Standard Gill versus Integral sensor time series (Figure 30) show a remarkable similarity between the two data sets. Vector-averaged wind speeds (Figures 31 and 32) agree to within 0.1 m/s, and the direction data (Figure 33) agree to within 1° at speeds above 5 m/s. The 0.5 m/s mean difference in direction is less than 1/2 bit of the compass and vane digital encoders. The slight curvature in the speed response indicates that the vector average wind speeds measured with the Integral system are smaller than those measured with the Standard system at speeds above 10 m/s.

A possible explanation is a small eddy-current damping effect on the anemometer due to the coupling between the magnet mounted on the shaft and the aluminum housing. The effect was tested for but not seen in simple lab tests which may not have detected a difference less than 1%.

Other possible explanations include differences in the wind sensors (considered unlikely since both systems use the same cup anemometer design) and differences in the system response due to the different wind direction sensors. We had gotten the visual impression during prelaunch dock testing of the C3 meteorological buoy that the shorter vane of the integral VAWR was more responsive to the wind fluctuations; however, spectra of the wind kinetic energy computed over periods of one month or longer with both the one hour time series and the 7 1/2 minute time series (Figure 34) show no significant basic differences in the frequency response of the two systems.

We then decided to look more closely at the basic 7 1/2 minute time series data and found that the shorter vane of the Integral system is more responsive at higher frequencies than the standard vane. To quantify this effect and also examine the initial assumption regarding the speed sensors, we have computed a variety of statistics using the 7 1/2 minute basic time series for the period May 1 through May 10 (Figures 35, 36 and Table III). The wind during this period (Figure 30) is predominately upwelling-favorable and relatively constant in direction except during a relaxation event on May 4 & 5, and the wind magnitude varies from less than 1 m/s during the relaxation event to greater than 15 m/s. Comparisons of the 7 1/2 minute vector average speeds (S) with the rotor speeds (R) in Figure 35 show that a) the two speed sensors agree on average to within 0.6 % at wind speeds of 10 m/s or greater, b) the difference in vector

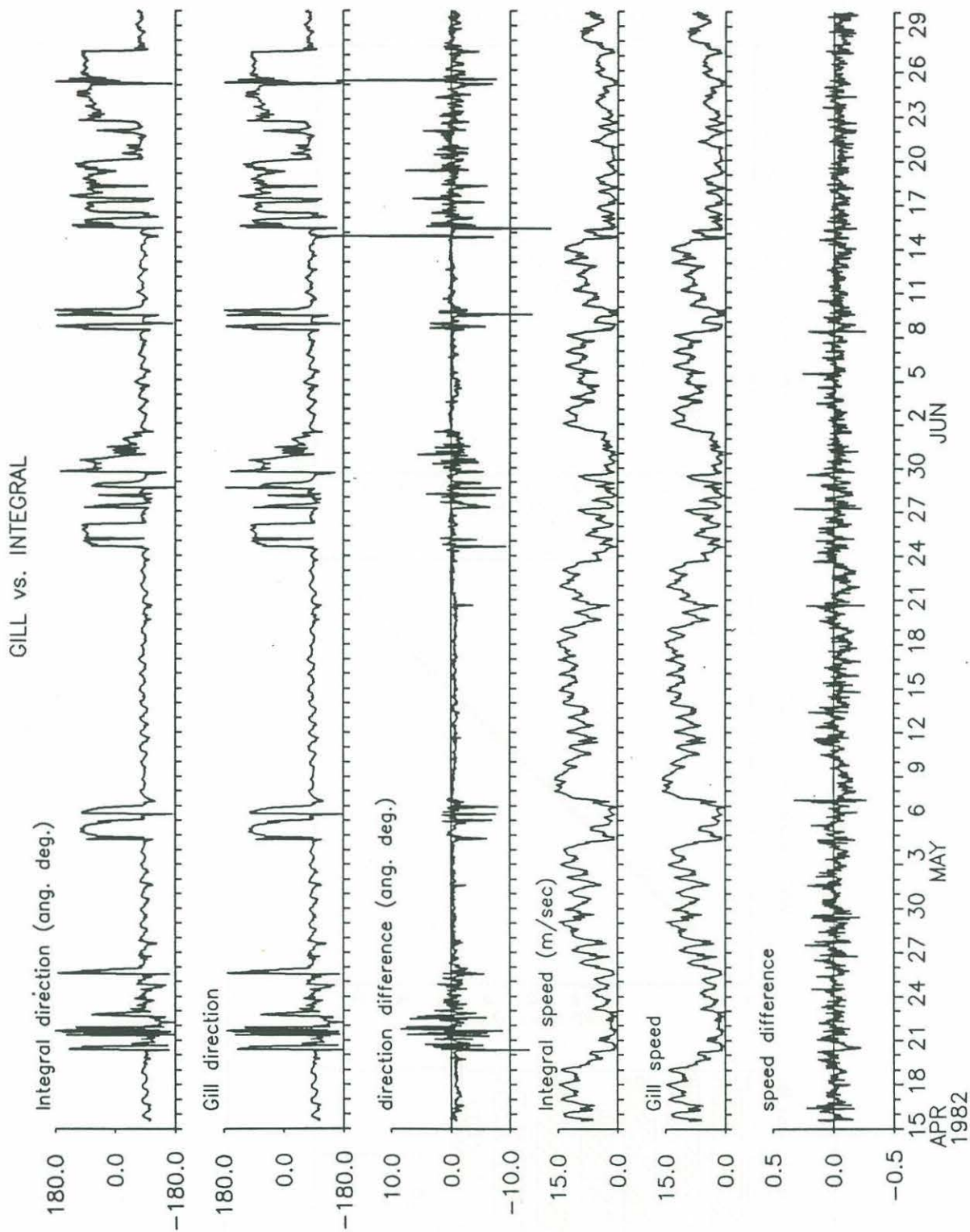


Figure 30. Time series of speed and direction (rotated into local geographic coordinates as defined in the text) for the VAWR with Gill wind sensor set, the VAWR with the Integral sensor set and the differences in the signals as measured by the two systems in CODE-2.

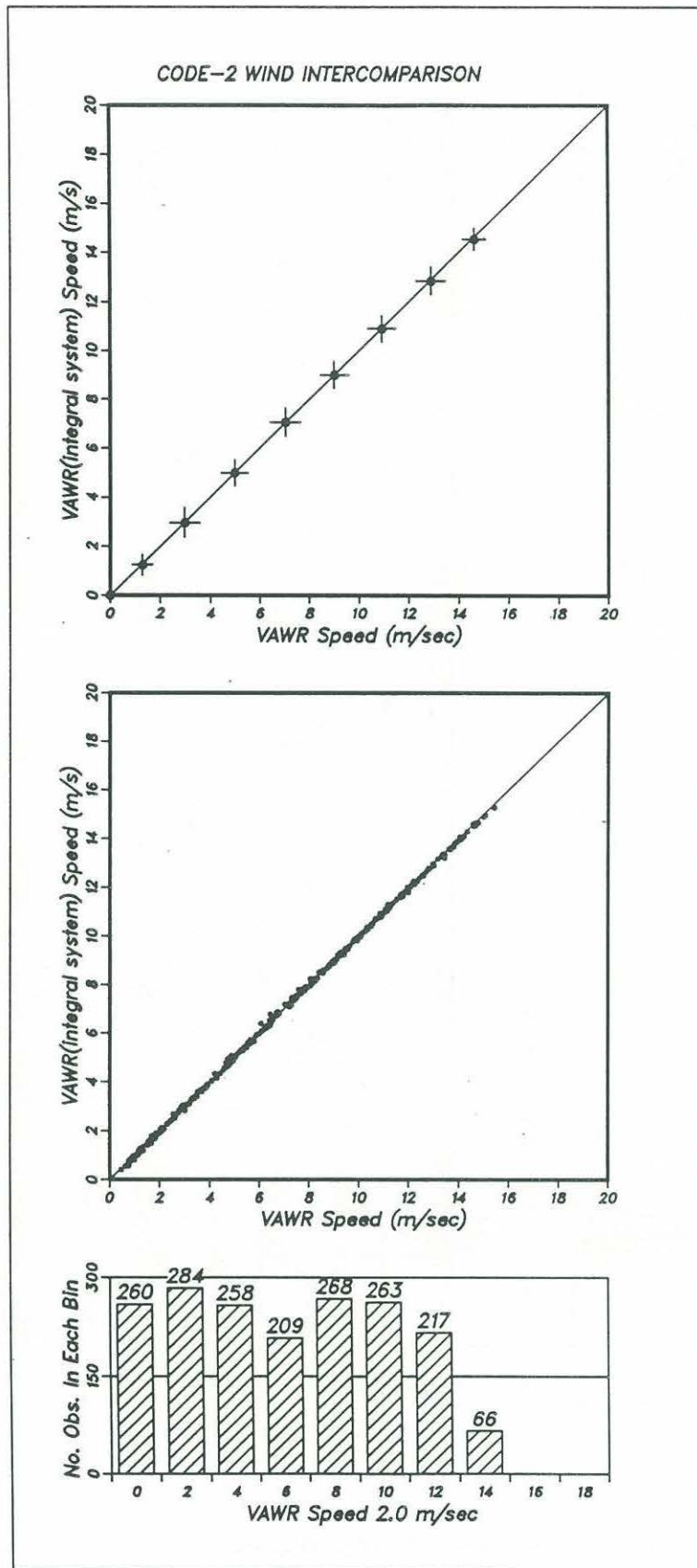


Figure 31. Histogram and scatter plots of the wind speed measurements made with the VAWR and Integral VAWR in CODE-2.

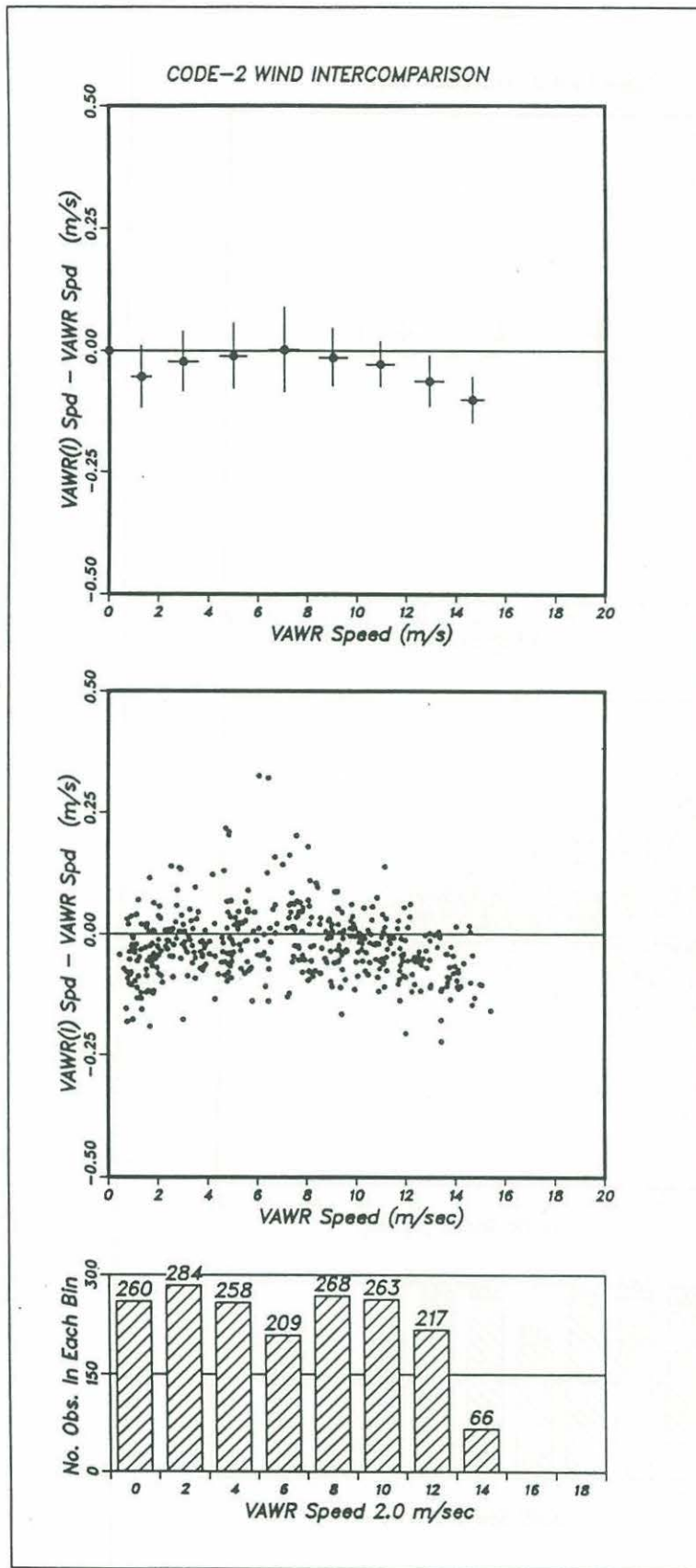


Figure 32. Histogram and plots of the VAWR and Integral VAWR speed difference versus wind speed in CODE-2.

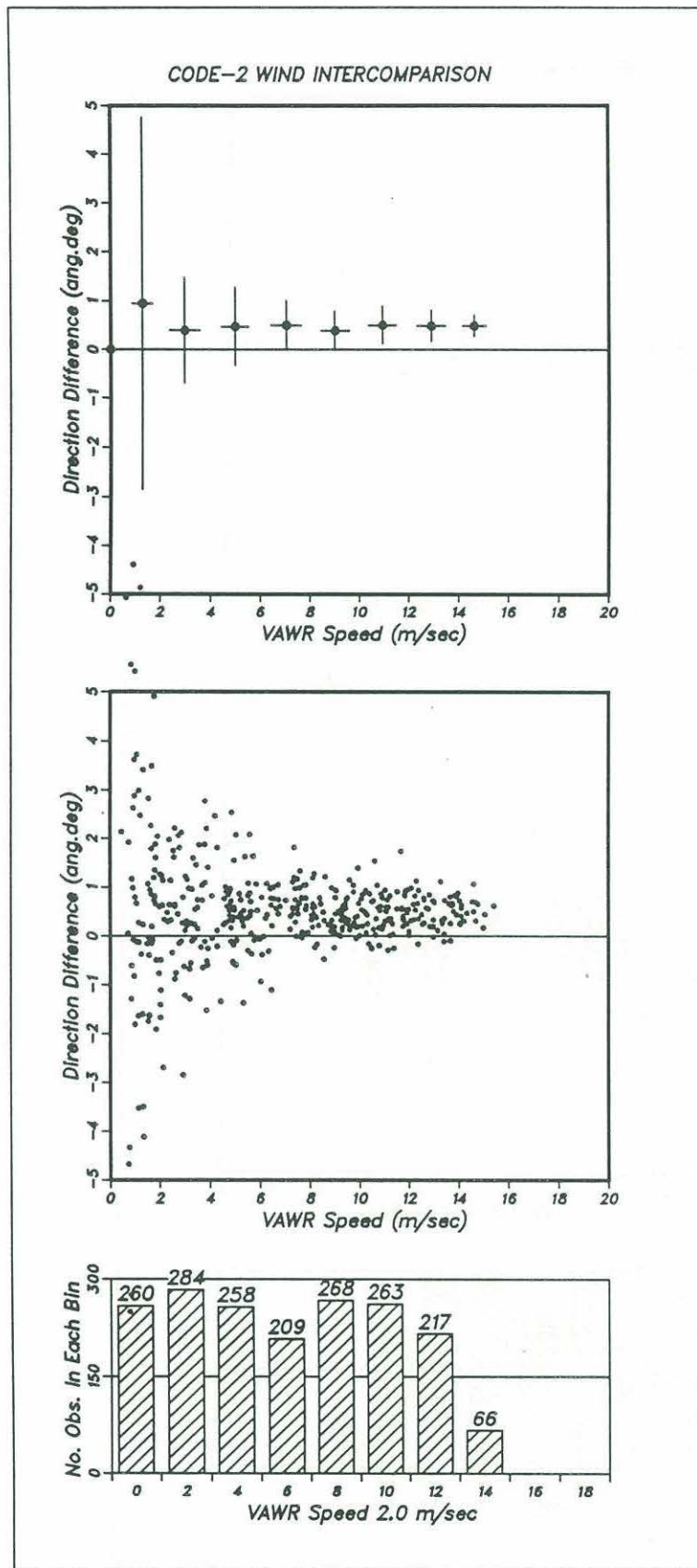


Figure 33. Histogram and plots of the direction differences versus wind speed for the VAWR and Integral VAWR in CODE-2.

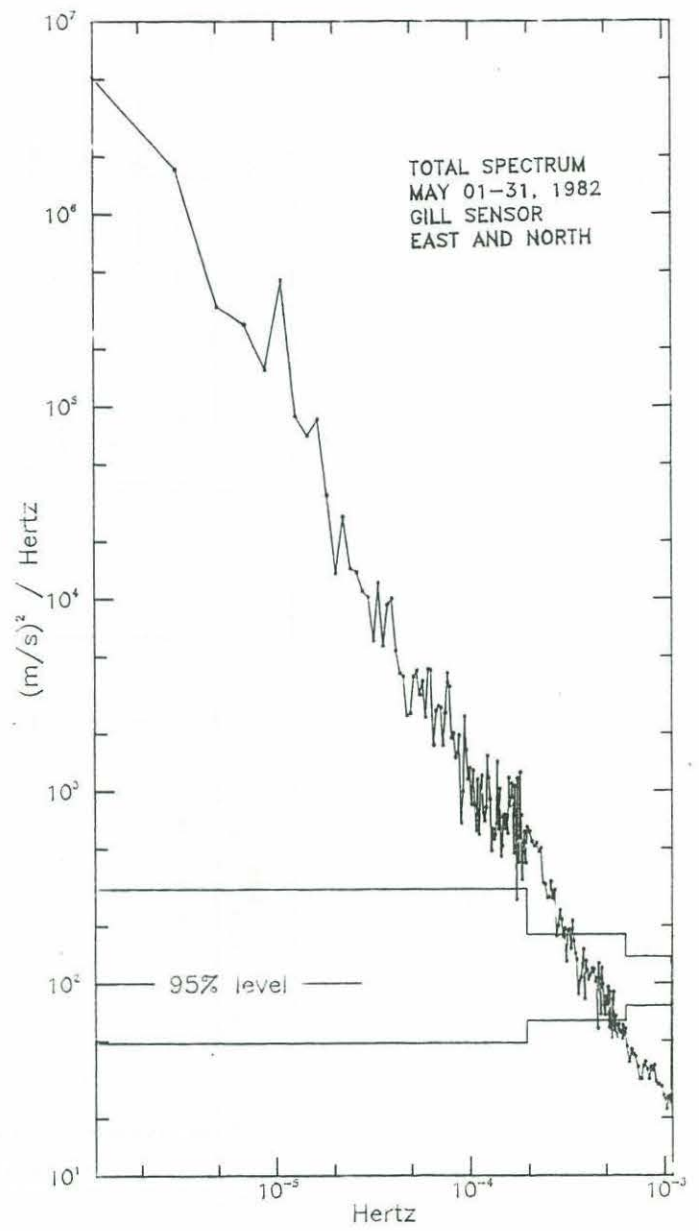
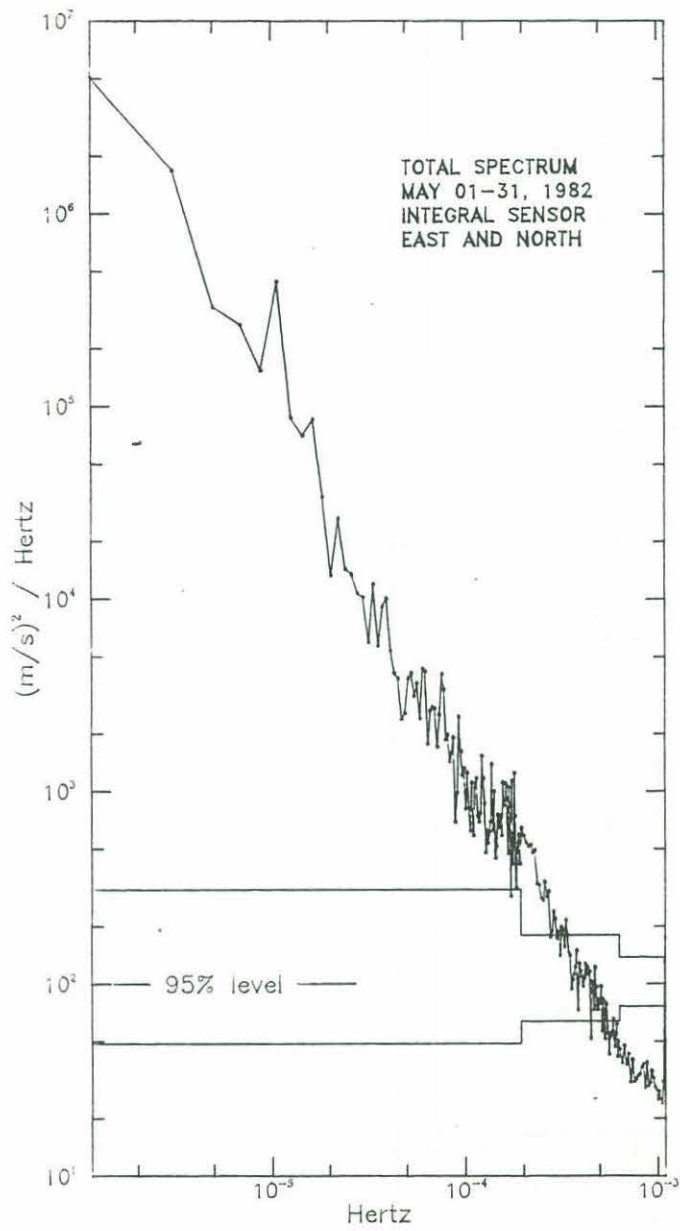


Figure 34. Frequency spectrum of a portion of the C3 VAWR wind record from CODE-2.

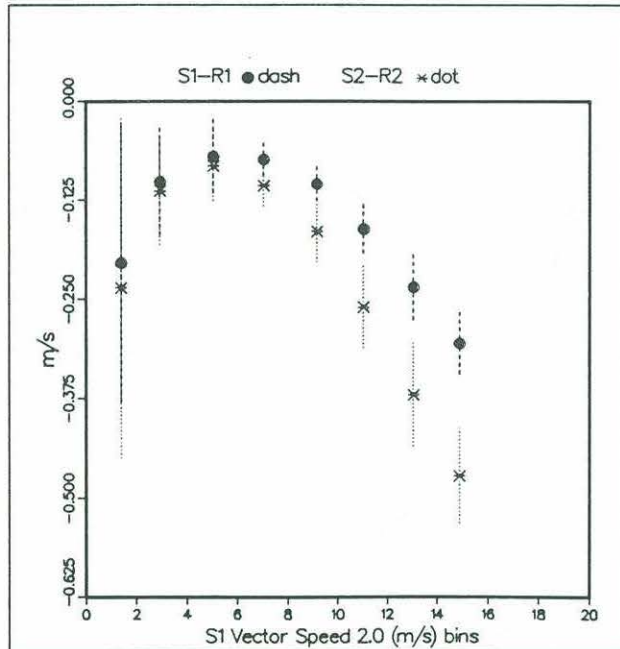
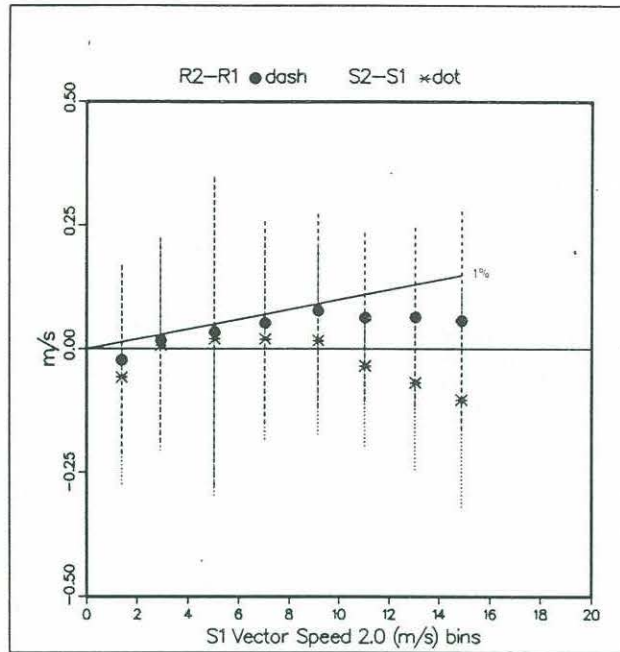


Figure 35. Plots of rotor speed difference ($R_2 - R_1$) and the vector-average speed difference ($S_2 - S_1$) versus wind speed (upper panel), and plots of the differences between vector-average speed (S) and rotor speed (R) for each instrument versus wind speed (lower panel). The subscripts 1 and 2 refer to the Standard and Integral VAWRs respectively. The mean and standard deviation statistics have been computed using a wind speed bin width of 2 m/s and the basic 7 1/2 minute time series for the 10 day period, May 1 through May 10, 1982.

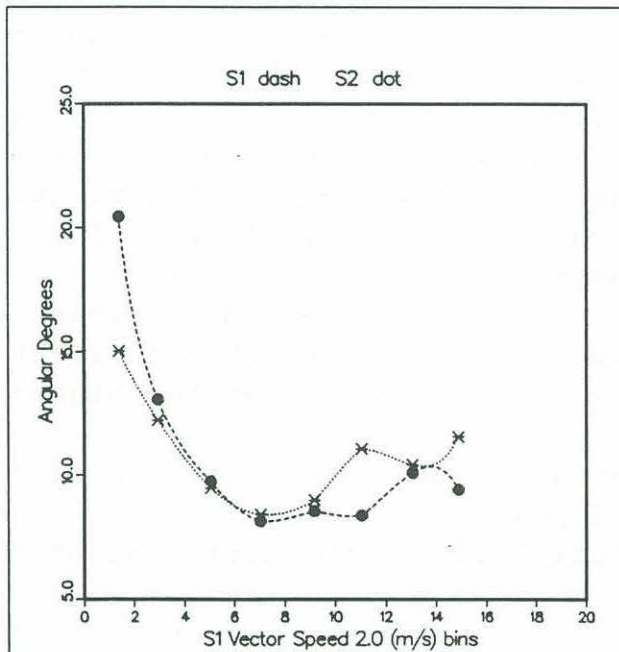
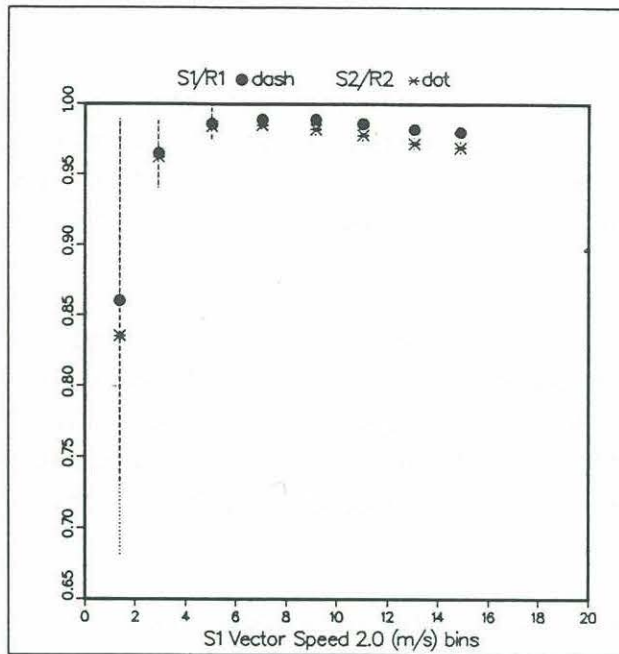


Figure 36. Plots of the ratio of vector-average speed to rotor speed for each instrument versus wind speed (upper panel) and the standard deviation of the instantaneous direction fluctuations versus wind speed (lower panel). As in Figure 35, subscripts 1 and 2 refer to the Standard and Integral VAWRs and the statistics have been computed for the time period May 1 - 10, 1982.

speeds based on the 7 1/2 minute and the one hour time series agree, and is slightly greater than the observed difference in rotor speeds, and c) the difference between rotor and vector speeds measured with the Integral system increases more rapidly with wind speed above 10 m/s.

This last result is clearly illustrated in plots of the ratio of vector-average speed to rotor speed (Figure 36). Above 10 m/s, the vector speed to rotor speed ratio for the Integral system decreases more rapidly with increasing wind speed indicating that the Integral system is measuring a greater variation in wind direction.

To estimate this effect, we have computed for each VAWR the instantaneous direction fluctuation θ' for each 7 1/2 minute period by subtracting the vector-average wind direction from the instantaneous wind direction recorded at the end of each 7 1/2 minute averaging period. While the resultant time series of θ' is clearly undersampled in time and does not resolve the 5 to 20 second variations due to wave and buoy motion and to the turbulence in the wind field, each 7 1/2 minute sample of θ' should be independent and the statistics of θ' during quasi-steady conditions should be representative of the actual behaviour of θ' . Plots of the standard deviation of the direction fluctuation (Figure 36) show a slight increase in θ' measured with the Integral system at the higher wind speeds.

If we assume that wind speed and direction fluctuations are statistically independent in quasi-steady conditions, then the average wind velocity (\bar{u}) in the direction of the mean wind (x) is simply

$$\bar{u} = \bar{s} \overline{\cos \theta'}$$

where \bar{s} is the average wind speed and $\overline{\cos \theta'}$ is the time average of the cosine of the instantaneous direction fluctuation, θ' .

To test this simple model, we have computed the ratio \bar{u}/\bar{R} and the time average of $\cos \theta'$ for the 24 hour period of May 8 when the winds were strong (14-16 m/s) and relatively constant in amplitude and direction. The results are: $\bar{u}/\bar{R} = 0.970 \pm 0.003$, $\overline{\cos \theta'} = 0.971 \pm 0.045$ (standard deviation $\theta' = 14.1^\circ$) for the Integral system and $\bar{u}/\bar{R} = 0.980 \pm 0.002$, $\overline{\cos \theta'} = 0.979 \pm 0.034$ (standard deviation $\theta' = 11.9^\circ$) for the Standard system. The good

agreement between \bar{u}/\bar{R} and $\bar{c}\bar{o}\bar{s}-\bar{\theta}^{\tau}$ during the stronger winds confirms that the small difference in measured vector-average wind speeds (Figures 32 and 35) is due primarily to the more responsive direction sensing of the Integral system.

8.2 Air temperature shields.

In CODE-1 meteorological buoys were outfitted with redundant temperature shields in order to determine which was the more effective shield for use over the ocean. By comparing night-time and daytime temperature differences, and assuming the radiation heating on both sensors was equal during the night-time, we could determine which shield was the more effective. Between CODE-1 and CODE-2, field tests were also run on Buzzards Bay with a newly constructed wind steered shield. Built of concentric tubes of surlyn, aluminum and pvc, the steered shield was designed as a wind vane and mounted to pivot with the wind and allow direct air flow across the temperature sensor (Figure 37). At the same time, the air flows freely between the tubes to carry away unwanted heat. This shield was compared to the multiplate Thaller shield in an attempt to evaluate the performance of the Thaller shield in the field.

After CODE-2, performance of the standard shield was tested in comparison with an R. M. Young aspirated temperature shield (Model No. 43404A) with a calibrated thermistor sensor. The Young shield was modified with a dc motor replacing the ac motor normally supplied with the unit and a reduced air flow resulted. Results of an eight day test from a Woods Hole dock are shown in Figure 38. The average difference over the record was $+0.06^{\circ}\text{C}$ with a standard deviation of 0.2° . The night-time average difference was -0.03°C with a standard deviation of 0.1° . Large errors occur when the wind speed is low, below about 2 m/s, and are most likely caused by solar heating during the daytime as the shield does not follow the wind, and by radiation heating of the aspirated standard (from the dock, buoy or ocean) at night. These tests are described in the WHOI Technical Report entitled "Air Temperature Shield Tests" by Payne (1987). Tests by the Atmospheric Environmental Service of Canada have shown the accuracy of an off-the-shelf R.M. Young shield (Model 43404A) to be 0.2°C RMS (Bob Young, Personal communication, 1988)

Although the temperature difference noted in CODE-1 resulted from several causes, the major heating contributor was the solar

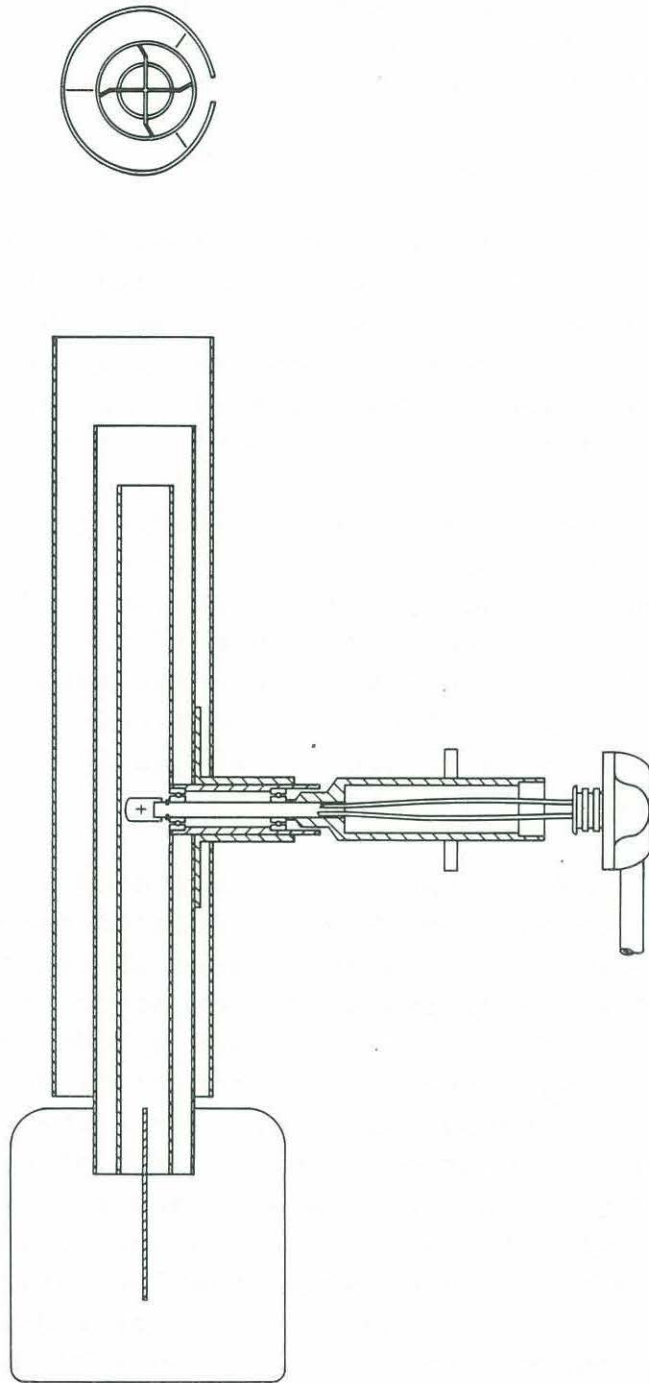


Figure 37. A naturally ventilated wind-steered radiation shield designed to provide a standard for comparisons of various radiation shields.

AT SHIELD INTERCOMPARISON

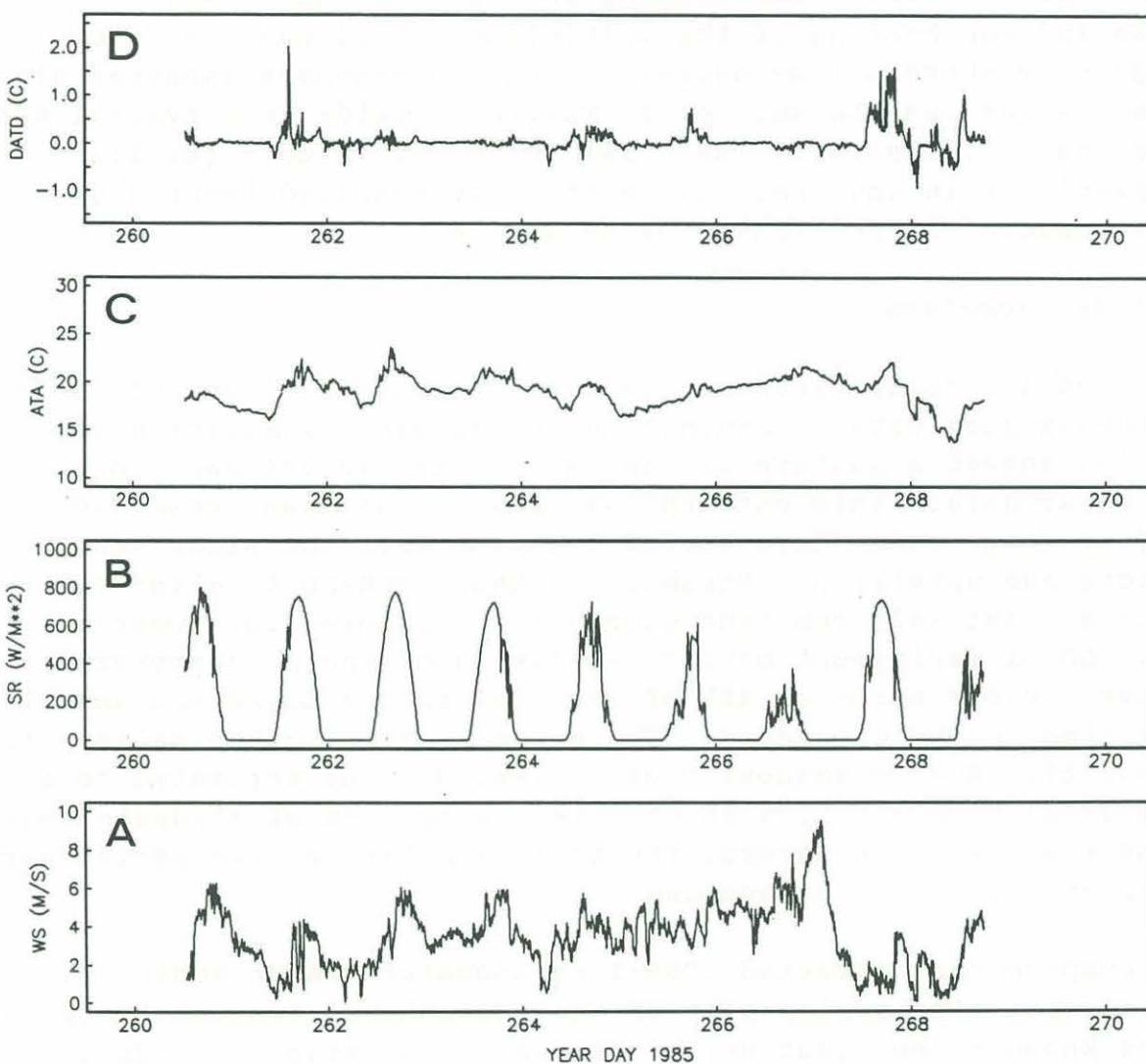


Figure 38. An eight-day test of radiation shields for air temperature sensors. Shown from bottom to top are time series of (A) air temperature, AT, as measured in the R. M. Young aspirated shield, (B) difference between AT and temperature sensed in the shield referred in the text as the steered shield, (C) wind speed and (D) insolation. (From Payne, 1987)

radiation. In general for wind speed greater than about 2 to 3 m/s, the temperature measured in the dome-shaped shield was warmer than that measured in the multiplate shield during the daytime by 0.5° or less. During the Buzzards Bay tests, the multiplate shield temperature was less than 0.2° warmer than the wind steered shield temperature for similar conditions. Thus, if the steered shield heating contribution was less than 0.1° , we conclude that the solar heating on the dome shield was 0.6° or less and the heating of the multiplate shield was 0.3° or less. Figure 39 shows a time series of the temperatures measured with the steered and the multiplate Thaller shields on a typical sunny day and a cloudy day. The noise on the difference results from variability in the temperature when the compared temperatures are not measured at precisely the same time.

8.3 Pyranometers.

In CODE-1, Eppley pyranometers deployed on the C3 and C5 buoys returned good data. Examination of the basic insolation time series showed a pattern of partial shading in the early morning on clear days. This pattern was rather consistent from day to day as clear sunny days tended to occur when the winds were strong and upwelling favorable and thus tending to align the buoy into a relatively constant geophysical orientation. Over the 108 day CODE-1 deployment period, shadowing of the pyranometer by other sensors occurred 48% of the time in the C3 record and 8% of the time in the C5 record. The maximum error in the daily total insolation due to shadowing on a clear day was estimated to be - 2.4% at C3 and - 1.5% at C5. As the pattern of shadowing was consistent in each record, the basic insolation time series were corrected for obvious shadows.

To compare the corrected CODE-1 pyranometer measurements, Figure 40 shows a time series plot of the atmospheric transmittance on days known to be clear using the basic insolation records and available satellite imagery. The atmospheric transmittance is defined here as the corrected daily total insolation divided by the insolation which would be measured if there was no atmosphere. The no-atmosphere insolation is a function of year day and latitude and has been computed using the subroutine "BSOLAR" supplied by R. E. Payne. Also plotted in Figure 39 is the computed clear-sky atmospheric transmittance based on the clear-sky insolation formula of the Smithsonian Astrophysical Tables. While pre-deployment dock tests indicated that the C5

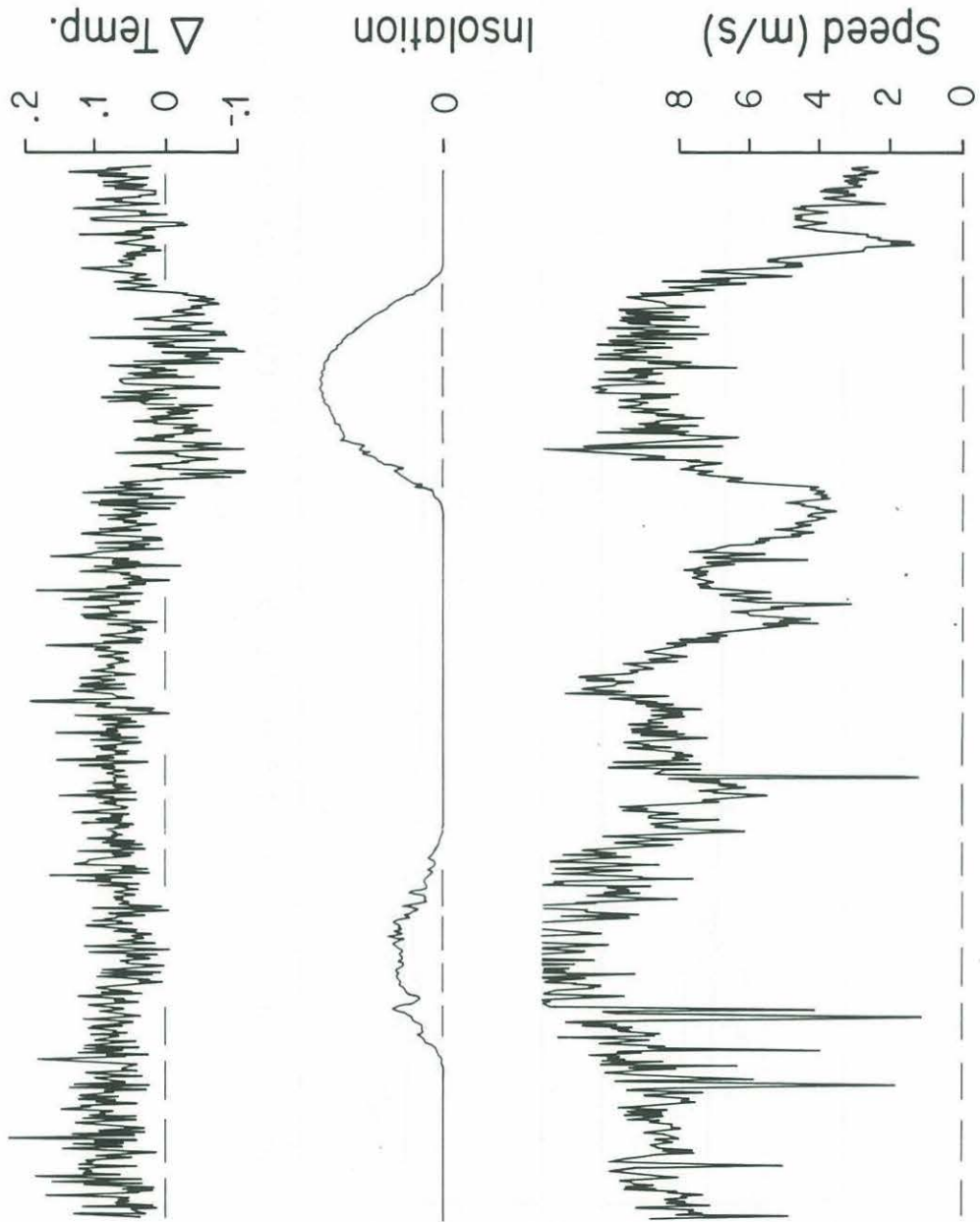


Figure 39. Difference plot of the temperatures measured in the standard shield and aluminum multiplate Thaller shield used in CODE. Wind speed, insolation and temperature difference are shown for a cloudy and a sunny day.

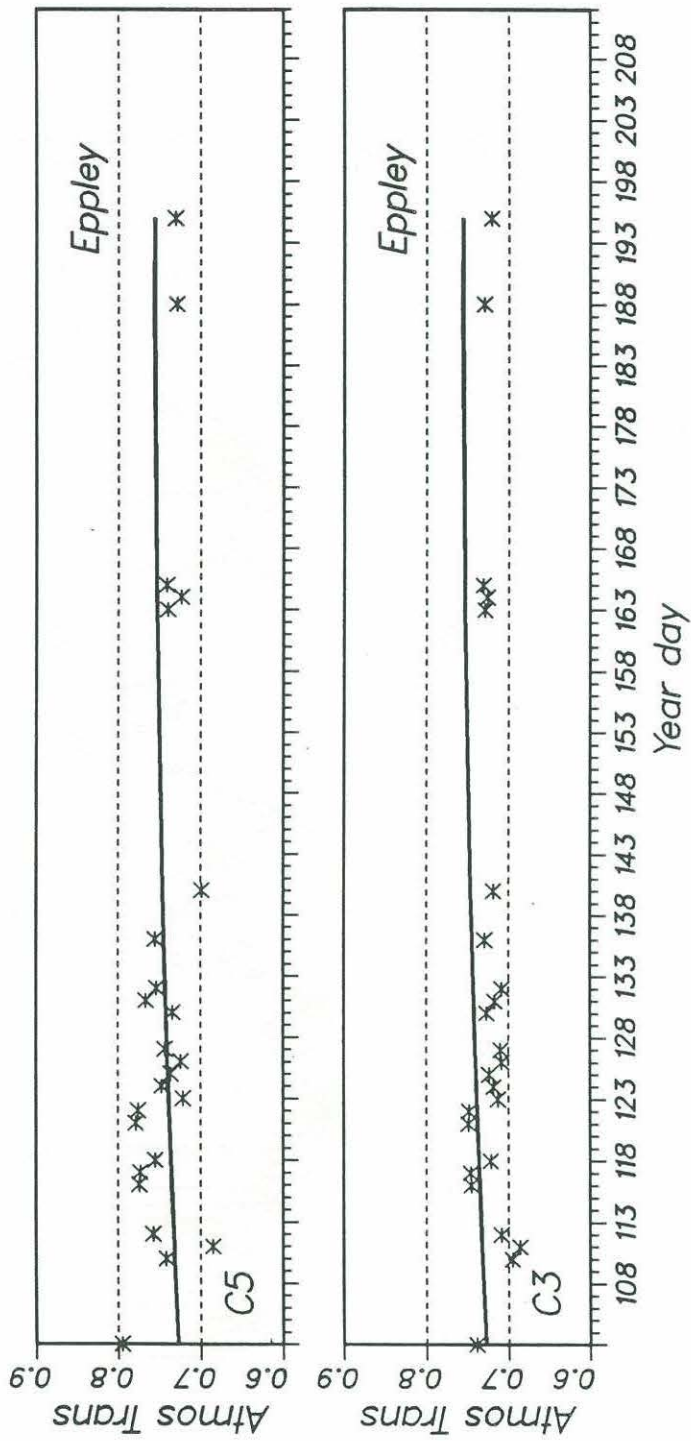


Figure 40. Theoretical and measured atmospheric transmittance based on the CODE-1 insolation data.

pyranometer read 5% higher than the C3 pyranometer, the clear-day atmospheric transmittance data shows that both Eppley pyranometers track well, and that the difference between the C5 and C3 systems is 2.6%, which is within the manufacturer's specification. Since we have no independent knowledge of the behavior of atmospheric transmittance, we cannot assess the question of sensor drift during CODE-1.

In CODE-2, one Eppley pyranometer deployed at C3 and three Hy-Cal pyranometers deployed at R2, N3, and R3 returned complete records. Examination of the basic insolation time series on clear days showed various degrees of early morning shadowing on clear days. The maximum error in the daily total insolation occurred in the N3 record. Again, since the pattern of shadowing was relatively consistent for each record, the basic insolation time series were corrected for obvious shadows. The corrected CODE-2 records were then used to compute atmospheric transmittance during clear days (Figure 40.) The C3 Eppley and C2 and R3 Hy-Cal pyranometers track well in time, showing a slow decrease in measured atmospheric transmittance during CODE-2 as was observed in CODE-1. The C3 Eppley and R3 Hy-Cal pyranometer records agree within a few percent while the C2 Hy-Cal pyranometer reads about 7% low in comparison with C3. The N3 Hy-Cal pyranometer exhibits more scatter in comparison to the other three sensors, and a larger decrease in atmospheric transmittance with time, suggesting a drift in sensor calibration. The N3 Hy-Cal pyranometer was recalibrated by the manufacturer in February 1984, and found to have a 7.5% decrease in sensitivity since its initial calibration in February 1982. The time series of Figure 41 suggests that some of this sensor drift occurred during the CODE-2 deployment.

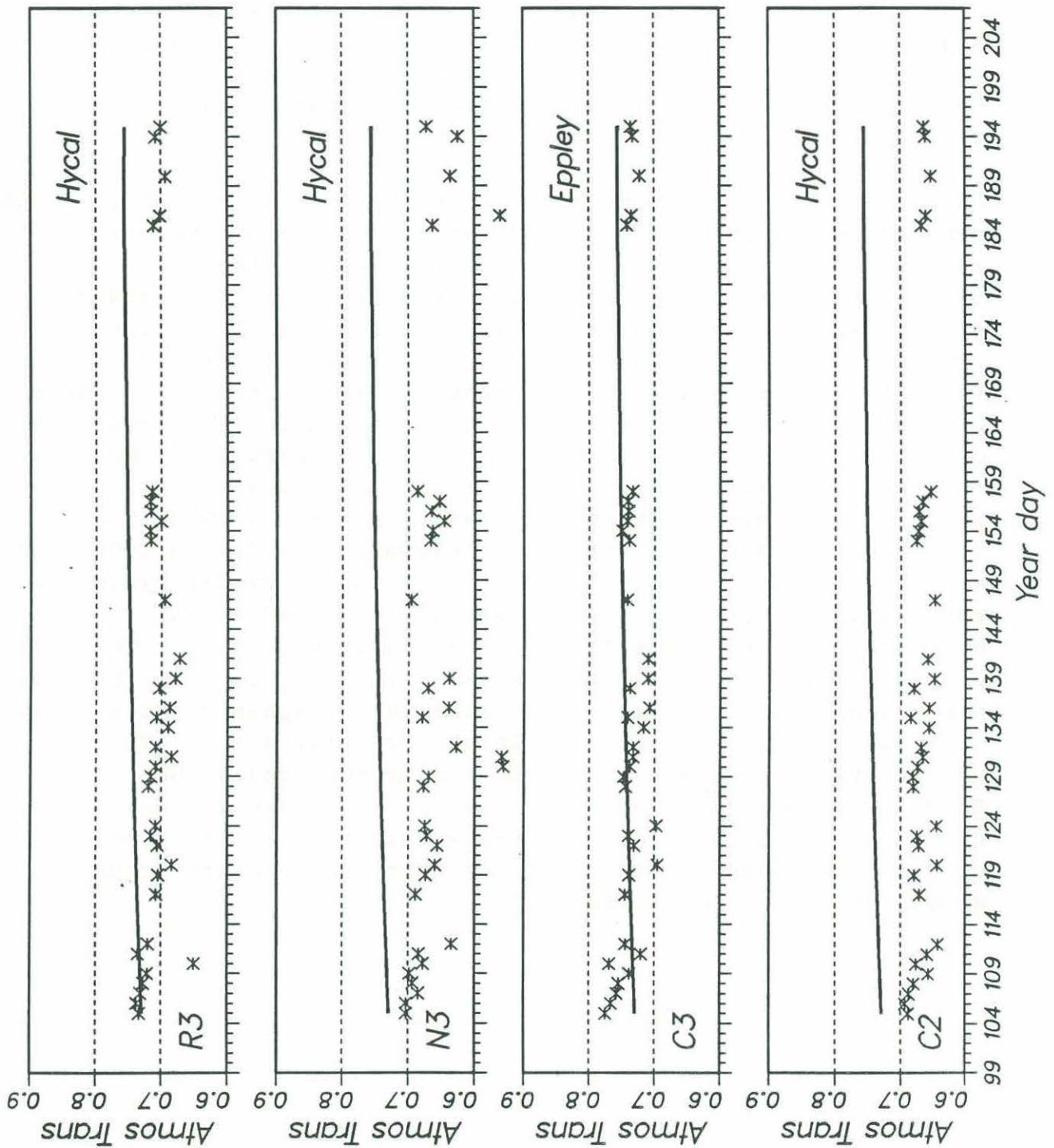


Figure 41. Theoretical and measured atmospheric transmittance based on the CODE-2 insolation data.

9. SYSTEM SPECIFICATIONS

The cassette tape recorder used in the VAWR will record data at a pre-set interval of any binary fraction of an hour from 2 hours to 1.76 seconds. The CODE VAWRs were set to record 8 times per hour, or 7.5 minutes. A VAWR (Wind, 2 temperatures, insolation and pressure) will record every 7 1/2 minutes for about 200 days with a 300 ft. tape. Standard VACM alkaline batteries will last about 200 days.

Listed in Table III are standard wind recorder specifications for the VAWR with 7 1/2 minute record interval. In some cases the resolution depends on this averaging (recording) interval.

Table III.

Sensor and System specifications for the CODE VAWRs

Wind Speed:

R. M. Young Anemometer # 6301

Threshold: 0.2 m/s
Range: 0.2 to 50 m/s
Sensor accuracy: 0.2 m/s
System accuracy: 0.2 m/s
Resolution: 0.375 meters of air
Distance Constant: 3.7 meters

Wind Direction relative to the instrument: (See note 1)

R. M. Young Wind-vane # 6101

Sensor accuracy: < 2.8 degrees (1 bit)
System accuracy: < 8.5 degrees
Resolution: 2.8 degrees (7 bit encoder)
Range: 0 - 360 degrees
Wind-vane delay distance: 1.2 meters

WHOI Integral vane (Custom)

Sensor accuracy: 2.8 degrees
System accuracy: < 8.5 degrees
Resolution: 2.8 degrees
Range: 0 - 360 degrees
Wind-vane delay distance: 0.75 meter
Vane-follower time constant: 1 second

TABLE III Continued.

Instrument Orientation :

EG&G compass # 55570

Linearity: < 5.6 degrees (2 bits)
System accuracy: < 8.5 degrees
Alignment: < 2.8 degrees (1 bit)
Resolution: 2.8 degrees (7 bit encoder)
Time Constant: 10 seconds

Sea temperature:

Thermometrics Thermistor # A118W-USSP100BA202XA1-A
(Probe # A667-USSP100BA202XA1-A)

Sensor accuracy: 0.003°C
System accuracy: 0.010°C
Resolution < 0.0002 °C
Range: -5 to +30°C
Thermal Time Constant: 7 sec

Air temperature:

YSI Thermistor # 44007 in WHOI Thaller Shield

Sensor accuracy: 0.2°C
System accuracy: 0.4°C (wind > 2 m/s)
Resolution: < 0.0002°C
Range: -10 to +35°C
Thermal Time Constant: 150 sec (in water)

Insolation: (See Note 2)

Eppley pyranometer # 8-48; Hy-Cal pyranometer # 8405:

Sensor accuracy: $\pm 3\%$ (42 W/m^2)
System Accuracy: < 5% (70 W/m^2)
Resolution: 0.003 W/m^2 (Eppley)
 0.01 W/m^2 (Hy-Cal)
Range: > 1394.6 W/m^2 (1 SC)
Time Constant: 3 to 4 seconds

Barometric pressure: (See Note 3)

Paroscientific pressure transducer # 215-AS-602

Sensor accuracy: 0.15 mbar (wind < 30 m/s)
System accuracy: 0.3 mbar
Resolution: 0.1 mbar
Range: 0 - 1034 mbar (0 - 15 psi.)
Over-pressure: 1.2 x FS (1240 mbar)
Null Stability: 0.016% / year
Thermal Stability: .0047% / °C

Relative Humidity: (See Note 4)

Hy-Cal relative humidity probe # HS-3552-B

Sensor accuracy: +6% RH
Resolution: .003% RH
Range: 0 - 100 % RH

Notes to Table III.

1. Direction accuracy given here is the sum of compass and wind-vane errors for the VAWR. Specifications such as those listed do not adequately describe the instrumentation; critical time varying inputs are often left unspecified. The platform motion may cause significant direction errors and must not be ignored in an error analysis. For example, the present VAWR compass has a 10 second time constant, meaning that the compass requires 10 seconds to fully respond to a step input. On an active buoy, the direction errors may be very large under certain conditions of non-symmetrical motions. The specifications listed are worse case totals, and better performance estimates may be determined from intercomparison tests such as those described in Section 8.

2. Accuracy specification assumes the sensor is horizontal (level).

3. It has been learned (1986) that the pressure transducers used in CODE exhibit a relatively large temporal and thermal drift in calibration. See the text for more detail (Section 6).

4. Accuracy quoted is the manufacturer's specification which was not verified in the field due to problems (see Section 7 of the text).

10. CONCLUSIONS

CODE and the VAWR represented renewed efforts at WHOI to make scientific quality meteorological measurements at sea. Building on the earlier work of Payne, Halpern and others, CODE began an era of wind measurements recently concluded with a 5-month deep ocean deployment of a 5 element moored array of meteorological buoys in FASINEX. By using the proven reliability of the VACM as a base, we successfully avoided most of the painful stage of implementing a newly developed instrument. The combination of the Gill-designed R. M. Young anemometer, the Integral vane and the Thaller shield has proved a rugged, reliable and accurate wind recorder for extended use at sea.

The Integral VAWR was used later in SEQUAL, TROPIC HEAT, LOTUS, MILDEX, and FASINEX. Two Standard VAWRs monitored the winds of the Strait of Gibraltar from a castle in Tarifa and a seaside knoll in Morocco. There have been lots of problems as well as successes and some of the things we have learned from the CODE and post-CODE deployments are briefly mentioned here for consideration in the development of an even better system of high quality at-sea moored meteorological measurements.

1. Wind sensors with "moving parts" do work for long periods at sea and are reliable. Control on the source of crucial components such as bearings must be carefully monitored.
2. Temperature shields are crucial, and measurements to $.05^{\circ}\text{C}$ are believed possible but not easy. The Thaller-type multi-plate shield is better than the dome shield, but for wind speeds below about 2 m/s, all naturally ventilated shields we tested fail. A wind-steered shield can be made which approaches the accuracy of an aspirated shield above speeds of 2 m/s. Water temperature measurements can be made 5 to 10 times more accurately.
3. Insolation data are crucial to heat flux calculations. Sensors must be gimballed if large errors due to buoy tilt are to be avoided. Improvements in pyranometer response (calibrations) are required. Fouling of glass domes does not appear to cause a problem at the $\pm 3\%$ accuracy level, but may be at the $\pm 1\%$ (10 W/m^2).
4. Transducers can be temporally and thermally unstable, performing as much as ten times worse than expected. There is little published long-term data on most newer sensor

designs. Manufacturers specifications, published data and reports cannot be trusted on face value. Frequent calibrations must be performed and a calibration history maintained on all sensors.

5. Humidity data (also crucial to heat flux calculations) continues to be elusive; this variable is the most difficult we attempt to measure and our record is poor.

11. ACKNOWLEDGMENTS

Our thanks go to the crew of the *R. V. Wecoma* and to the WHOI Buoy Group personnel who deployed and recovered the VAWR systems. They only once wiped out a complete sensor set with a single swipe of the medicine ball (but after all "That's why we carry spares"). The success of the VAWR used in CODE was due in large measure to the work of Joe Poirier, dedicated electronics technician and our current meter shop supervisor. He modified the VACMs then personally took the VAWR under his wing and made sure it worked. The continuing success is due to Joe and to Craig Marquette, who helps to insure the proper mating of the instrument to the buoy. Thanks to Dick Limeburner for support all along, to Carol Alessi, Jane Louise and Barbara Gaffron for help with the data plots and manuscript, to Bob Weller and Dick Payne for lots of helpful advice and to Bob Young for his willing cooperation.

However, the largest debt of gratitude we owe to Gerry Gill, whose name is synonymous with quality meteorological measurements. More than anything, Gerry taught us the importance of the interface between the sensors and the REAL world. In addition, we borrowed from his careful designs the wind sensors, radiation shields for the air temperature and humidity sensors and the atmospheric pressure port. Thank you, Gerry Gill.

Funding for this work was provided by the National Science Foundation through grants OCE 80-14941 and OCE 84-17769.

This is CODE Technical Report No. 44.

12. REFERENCES

Allen, J. S., R. C. Beardsley, W. S. Brown, D. A. Cacchione, R. E. Davis, D. E. Drake, C. Friehe, W. D. Grant, A. Huyer, J. D. Irish, M. M. Janopaul, A. J. Williams III and C. D. Winant, 1982. A preliminary description of the CODE-1 field program. Woods Hole Oceanographic Institution Technical Report, *WHOI-82-51*, CODE Technical Report No. 9. 47 pp.

Busch, N. E., O. Cristensen, L. Kristensen, L. Lading and S. E. Larsen, 1980. Cups, vanes, propellers, and laser anemometers. In *Air Sea Interaction Instruments and Methods*, edited by F. Dobson, L. Hasse and R. Davis, 801 pp., Plenum Press, London.

CODE Group, 1983. Coastal Ocean Dynamics Experiment (CODE): A preliminary program description. *EOS Transactions AGU*, 64, 538-540.

Friehe, Carl A., Robert C. Beardsley, Clinton D. Winant and Jerome P. Dean, 1984. Intercomparison of aircraft and surface buoy meteorological data during CODE-1. *Journal of Atmospheric and Oceanic Technology*, 1, 79-86.

Gill, Gerald C., 1976. Development and testing of a no-moving-parts static pressure inlet for use on ocean buoys. Report on research sponsored by the NOAA Data Buoy Office, Bay St. Louis, Mississippi, 43 pp., 48 figures.

Gill, Gerald C., 1979. Development of a small rugged radiation shield for air temperature measurements on drifting buoys. Report on research sponsored by NOAA Data Buoy Office, Bay St. Louis, Mississippi, 23 pp., 17 figures.

Halpern, D., 1974. Observations of the deepening of the wind-mixed layer in the northeast Pacific Ocean. *Journal of Physical Oceanography*, 4, 454-466.

Katsaros, Kristina B. and John E. DeVault, 1986. On Irradiance measurement errors at sea due to tilt of pyranometers, *Journal of Atmospheric and Oceanic Technology*, 3, 740-745.

Limeburner, Richard, 1985. CODE-2: Moored array and large-scale data report. Woods Hole Oceanographic Institution Technical Report *WHOI 85-35*, CODE Technical Report No. 38, 234 pp.

- MacCredy, Paul B. and Henry R. Rex, 1964. Response characteristics and meteorological utilization of propeller and vane wind sensors. *Journal of Applied Meteorology*, 3, 182-193.
- McCullough, James R., 1975. Vector averaging current meter speed calibration and recording technique. Woods Hole Oceanographic Institution Technical Report *WHOI-75-44*, 35 pp.
- Mooers, C. N. K., 1973. A technique for the cross-spectrum analysis of pairs of complex-valued time series, with emphasis on properties of polarized components and rotational invariants. *Deep-Sea Research*, 20, 1129-1141.
- Payne, R. E., 1974. A buoy-mounted meteorological recording package. Woods Hole Oceanographic Institution Technical Report, *WHOI-74-40*, 31 pp.
- Payne, Richard E., 1981. Performance characteristics of some wind sensors. Woods Hole Oceanographic Institution Technical Report, *WHOI-81-101*, 48 pp.
- Payne, Richard E., 1987. Air temperature shield test. Woods Hole Oceanographic Institution Technical Report, *WHOI-87-40*, 22 pp.
- Rosenfeld, Leslie K., Editor, 1983. CODE-1 Moored array and large-scale data report. Woods Hole Oceanographic Institution Technical Report *WHOI 82-23*, CODE Technical Report No. 21, 185 pp.
- Weller, Robert A., Richard E. Payne, W. G. Large and Walter Zenk, 1983. Wind measurements from an array of oceanographic moorings and from F/S Meteor during JASIN. *Journal of Geophysical Research*, 88, No. C14, 9689-9705.
- Weast, Robert C., Editor, 1980 *Handbook of Chemistry and Physics* 61st Edition, CRC Press, Boca Raton, Florida

DOCUMENT LIBRARY

August 21, 1987

Distribution List for Technical Report Exchange

Attn: Stella Sanchez-Wade
Documents Section
Scripps Institution of Oceanography
Library, Mail Code C-075C
La Jolla, CA 92093

Hancock Library of Biology &
Oceanography
Alan Hancock Laboratory
University of Southern California
University Park
Los Angeles, CA 90089-0371

Gifts & Exchanges
Library
Bedford Institute of Oceanography
P.O. Box 1006
Dartmouth, NS, B2Y 4A2, CANADA

Office of the International
Ice Patrol
c/o Coast Guard R & D Center
Avery Point
Groton, CT 06340

Library
Physical Oceanographic Laboratory
Nova University
8000 N. Ocean Drive
Dania, FL 33304

NOAA/EDIS Miami Library Center
4301 Rickenbacker Causeway
Miami, FL 33149

Library
Skidaway Institute of Oceanography
P.O. Box 13687
Savannah, GA 31416

Institute of Geophysics
University of Hawaii
Library Room 252
2525 Correa Road
Honolulu, HI 96822

Library
Chesapeake Bay Institute
4800 Atwell Road
Shady Side, MD 20876

MIT Libraries
Serial Journal Room 14E-210
Cambridge, MA 02139

Director, Ralph M. Parsons Laboratory
Room 48-311
MIT
Cambridge, MA 02139

Marine Resources Information Center
Building E38-320
MIT
Cambridge, MA 02139

Library
Lamont-Doherty Geological
Observatory
Columbia University
Palisades, NY 10964

Library
Serials Department
Oregon State University
Corvallis, OR 97331

Pell Marine Science Library
University of Rhode Island
Narragansett Bay Campus
Narragansett, RI 02882

Working Collection
Texas A&M University
Dept. of Oceanography
College Station, TX 77843

Library
Virginia Institute of Marine Science
Gloucester Point, VA 23062

Fisheries-Oceanography Library
151 Oceanography Teaching Bldg.
University of Washington
Seattle, WA 98195

Library
R.S.M.A.S.
University of Miami
4600 Rickenbacker Causeway
Miami, FL 33149

Maury Oceanographic Library
Naval Oceanographic Office
Bay St. Louis
NSTL, MS 39522-5001

REPORT DOCUMENTATION PAGE	1. REPORT NO. WHOI-88-20	2.	3. Recipient's Accession No.
4. Title and Subtitle A Vector-Averaging Wind Recorder (VAWR) System for Surface Meteorological Measurements in CODE (Coastal Ocean Dynamics Experiment)		5. Report Date May 1988	
7. Author(s) Jerome P. Dean and Robert C. Beardsley		8. Performing Organization Rept. No. WHOI-88-20	
9. Performing Organization Name and Address The Woods Hole Oceanographic Institution Woods Hole, Massachusetts 02543		10. Project/Task/Work Unit No.	
		11. Contract(C) or Grant(G) No. (C) (G) OCE 80-14941 OCE 84-17769	
12. Sponsoring Organization Name and Address The National Science Foundation		13. Type of Report & Period Covered Technical Report	
		14.	
15. Supplementary Notes This report should be cited as: Woods Hole Oceanog. Inst. Tech. Rept., WHOI-88-20.			
16. Abstract (Limit: 200 words) As part of the Coastal Ocean Dynamics Experiment (CODE) field program, moored buoys were instrumented to measure and record wind speed and direction, air and water temperature, insolation, barometric pressure and relative humidity. Appropriate sensors were selected, necessary modifications to the sensors and existing current meters were made, and Vector Averaging Wind Recorders (VAWRs) were assembled. R. M. Young utility rotor and vane wind sets designed by G. Gill, Paroscientific Digiquartz pressure sensors, Eppley pyranometers and Hy-Cal relative humidity and solar sensors were used in two field experiments. Standard VACM direction and temperature sensors were maintained in the wind recorders. Devices were constructed as needed to protect against measurement errors due to wind, sun and ocean spray. Four WHOI VAWRs with Gill wind sensor sets were deployed CODE-1 in 1981. Seven VAWRs were deployed in CODE-2 in 1982. A modified VMCM (Vector Measuring Current Meter) was used for comparison in CODE-1, and the seventh VAWR deployed in CODE-2 carried an integral sensor set for comparison. Although several VAWRs had minor problems, all but one VAWR in the two experiments returned useful scientific data.			
17. Document Analysis a. Descriptors 1. Marine Meteorology 2. Sensor Comparisons 3. Moored Instrumentation b. Identifiers/Open-Ended Terms c. COSATI Field/Group			
18. Availability Statement Approved for publication; distribution unlimited.		19. Security Class (This Report) UNCLASSIFIED	21. No. of Pages 74
		20. Security Class (This Page)	22. Price

